Macroscopic delayed choice and retrocausality: Quantum eraser, Leggett-Garg, and dimension witness tests with cat states

Manushan Thenabadu and M. D. Reid
Centre for Quantum Science and Technology Theory, Swinburne University of Technology, Melbourne 3122, Australia

(Received 25 September 2021; revised 3 January 2022; accepted 26 January 2022; published 8 June 2022)

We propose delayed-choice experiments carried out with macroscopic qubits, realized as macroscopically distinct coherent states $|\alpha\rangle$ and $|-\alpha\rangle$. Quantum superpositions of $|\alpha\rangle$ and $|-\alpha\rangle$ are created via a unitary interaction $U(\theta)$ based on a nonlinear Hamiltonian, in analogy with polarizing beam splitters used in photonic experiments. Macroscopic delayed-choice experiments give a compelling reason to develop interpretations not allowing macroscopic retrocausality: This would otherwise suggest changes to the macroscopic qubit value based on a future measurement setting ϕ. We therefore consider weak macroscopic realism (wMR), which for the system at time t specifies a hidden variable λ_θ to determine the macroscopic qubit value, independently of ϕ. Using entangled cat states, we demonstrate a quantum eraser where the choice to measure a which-way or wave-type property is delayed. Consistency with wMR is possible, if we interpret the macroscopic qubit value to be determined by λ_θ without specification of the state at the level of $\hbar$. We then demonstrate violations of a delayed-choice Leggett-Garg inequality, and of the Wheeler-Chaves-Lemos-Pienaar dimension witness inequality, for the macroscopic qubits. This negates all two-dimensional nonretrocausal wMR models. However, one can interpret consistently with wMR, thus avoiding conclusions of macroscopic retrocausality, by noting extra dimensions, and that violations require further unitary dynamics U after t. The violations are then explained as failure of deterministic macroscopic realism, which specifies the validity of λ_θ *prior* to the dynamics $U(\theta)$ determining the measurement setting θ. Finally, although there is consistency with wMR for macroscopic observations, Einstein-Podolsky-Rosen–type paradoxes pointing to the incompleteness of quantum mechanics exist at a microscopic level, based on fringe distributions.

DOI: 10.1103/PhysRevA.105.062209

I. INTRODUCTION

Gedanken experiments involving a delayed choice of measurement motivated Wheeler and others to consider whether quantum mechanics implies failure of realism, or else retrocausality [1–3]. The argument is often presented for the two-slit experiment, where a photon travels through the slits exhibiting either particlelike or wavelike behavior. The observation of an interference pattern is interpreted as wavelike behavior; the observation that the photon traveled along a single path is interpreted as particlelike behavior. A similar argument exists for a Mach-Zehnder (MZ) interferometer, where the photon travels in one or other path associated with the outputs of a beam splitter [1,2]. In the delayed-choice quantum eraser [4], the decision to observe either the wavelike or particlelike behavior is delayed until after the photon has passed through the apparatus, and the fringe distribution vanishes or emerges, conditionally on the measurement made at the later time. Thus, there is an apparently paradoxical situation whereby it seems as though whether the photon went through "both slits" or "one slit" can be changed by an event (the choice of measurement) in the future.

Multiple different refinements and interpretations have been given [3,5–27], but the consensus is that the original delayed-choice experiments do not imply the need for retrocausality. The above paradox arises only if one views the system as being either a wave or particle. The work of Ionicioiu and Terno proposed a quantum beam splitter [19], which would place the system in a quantum superposition of wavelike and particlelike states. An intermediate regime can be quantified, and a class of hidden variable theories based on the assumption of either wavelike or particlelike behavior can be negated [19,20]. Significantly, Chaves, Lemos, and Pienaar (CLP) resolved these issues further by constructing a two-dimensional causal model for the MZ delayed-choice experiment [27], thus ruling out any need for retrocausal explanations.

On the other hand, with the inclusion of an additional phase shift in the MZ interferometer, CLP demonstrated that a two-dimensional classical model would need to be retrocausal in order to explain the predicted observations, which imply violation of a dimension witness inequality [27]. Recent experiments confirm these predictions [28–30]. In their analysis, "nonretrocausal" implies that, in a model which assumes realism, hidden variables λ associated with the preparation state are independent of any future measurement setting ϕ. La Cour and Yudichak recently presented a model which is nonretrocausal, but possesses extra dimensions [18]. Their model is based on stochastic electrodynamics, which is not generally equivalent to quantum mechanics.

In this paper, we propose and analyze *macroscopic* versions of delayed-choice experiments. Our results demonstrate

that delayed-choice paradoxes and the causal-modeling tests of CLP are evident at a macroscopic level, beyond $\hbar$, without the need for a microscopic resolution of measurement outcomes. Since retrocausality is more paradoxical at a macroscopic level, we argue that this strengthens the need to explain the results of the experiments without invoking retrocausality.

Specifically, we follow [31–33] and map from a microscopic to a macroscopic regime, where spin qubits $|\uparrow\rangle$ and $|\downarrow\rangle$ are realized as macroscopically distinct coherent states $|\alpha\rangle$ and $|-\alpha\rangle$ (α is large), that form a macroscopic qubit. The qubit values S of $+1$ and -1 corresponding to the coherent states $|\alpha\rangle$ and $|-\alpha\rangle$ can be distinguished by a measurement of the field quadrature amplitude X, without the need to resolve at the level of $\hbar$. In analogy with a polarizing beam splitter (PBS) used in the photonic experiments, superpositions of the two coherent states (called cat states) [31–34]

$$\cos\theta|\alpha\rangle + i\,\sin\theta|-\alpha\rangle \tag{1}$$

can be created using a unitary interaction $U(t) \equiv U(\theta)$ based on a nonlinear Hamiltonian $H_{\rm NL}$. The value of t determines θ and hence the probability amplitudes of the two-state superposition. This provides a mechanism for a direct mapping from the microscopic to macroscopic delayed-choice experiments.

To analyze quantitatively, we seek to define *macroscopic retrocausality*. In analyses of delayed-choice experiments, the meaning of retrocausality is intertwined with that of realism. Following Leggett and Garg [35], we therefore consider macroscopic realism: *Macroscopic realism* (MR) asserts a predetermination of the outcome S of the measurement of the macroscopic qubit value (the sign of X), for the system prepared at time t_M in a superposition (1). In a MR model, a hidden variable λ_M exists to describe the macroscopic state of the system at the time t_M, meaning that its value gives the outcome S of the macroscopic qubit measurement. Since the value does not require a microscopic resolution, the validity of λ_M is a *very weak* assumption (i.e., is more strongly justified) compared to the assumption of hidden variables made in the original delayed-choice proposals, or in Bell's theorem [36], where measurements must distinguish microscopic states. The advantage of the cat-state analysis is that it is based on macroscopic as opposed to microscopic realism.

However, recent work establishes the need to carefully consider whether the unitary rotation $U(\theta)$ associated with the measurement setting θ has been performed prior to t_M, or not. This leads to two definitions of macroscopic realism: *deterministic macroscopic realism* (dMR) and *weak macroscopic realism* (wMR) [32,33]. Deterministic macroscopic realism asserts a predetermination of outcomes, at a time t, for multiple future choices of θ (e.g., θ_1 and $\theta_2 = \phi$), so that these outcomes are given by multiple hidden variables (e.g., λ_1 and λ_2) simultaneously specified at t. Deterministic macroscopic realism is falsifiable for cat states [32,33].

To define macroscopic retrocausality, we therefore consider weak macroscopic realism (wMR) [33]: Weak macroscopic realism asserts that the system prepared at time t_M in a superposition (1) is in a state giving a definite outcome λ_M (λ_M being $+1$ or -1) for the macroscopic pointer qubit measurement S. It is implicit as part of the definition that the value λ_M be independent of any future measurement setting ϕ. We use the term *pointer measurement* because it is assumed that the unitary rotation $U(\theta)$ determining the measurement setting has already been performed, *prior* to t_M, i.e., the system has been prepared in the appropriate basis.

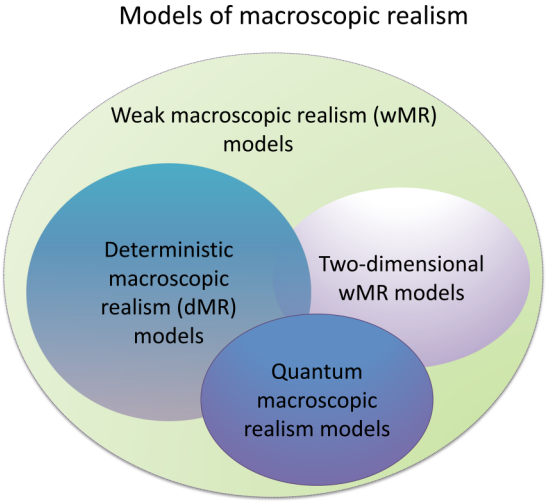

FIG. 1. Venn diagram showing the different models of macroscopic realism (MR). The superset consists of all weak macroscopic realism models (wMR). The three models (dMR, quantum macroscopic realism models, and two-dimensional wMR models) that are subsets are predicted to be ruled out by the experiments proposed in this paper.

The main results of this paper are threefold: First, we demonstrate the possibility of performing macroscopic delayed-choice tests using cat states. We consider three tests: the quantum eraser, a delayed-choice Leggett-Garg test, and a CLP violation of the dimension witness inequality. By examining the unitary dynamics $U(t)$, it is shown that at certain times t_M the assumption of λ_M is relevant because the system is in a two-state macroscopic superposition (1). The results give paradoxes suggesting macroscopic retrocausality.

Second, we explain how these predictions can be viewed consistently with wMR, thus providing a counter argument to any conclusions of macroscopic retrocausality. During the dynamics, the state of the system has a more general form than (1) and extra dimensions are evident in the quantum continuous-variable phase-space representations. It is possible to argue consistently within the framework of CLP framework that λ_M is valid at the time t_M, and hence that there is no macroscopic retrocausality. Instead, the violations of the dimensions witness and delayed-choice Leggett-Garg inequalities reflect the extra dimensions and the failure of dMR, which (it is argued) arises from failure of Bell-type hidden variables defined microscopically.

Lastly, we point out Einstein-Podolsky-Rosen (EPR) type paradoxes [33,37] giving inconsistencies with the completeness of quantum mechanics at a microscopic level (where fringes in the distributions are evident), *if* one assumes the validity of wMR. This allows a negation of a class of models, which we refer to as quantum MR models. The conclusions regarding negation of the different models of macroscopic realism are summarized in Fig. 1.

Layout of paper. The paper is organized as follows. In Secs. III–VI, we propose four experiments. In Sec. II we first summarize the different models of macroscopic realism examined in this paper, and give an overview of the conclusions about which models are negated based on the predictions for the four experiments.

In Sec. III, we propose a quantum eraser experiment using cat states. In analogy with quantum eraser experiments based on entangled states [3,7,24], the system is prepared at $t_1 = 0$ in a two-mode entangled cat state $\sim|\alpha\rangle_a|-\beta\rangle_b - |-\alpha\rangle_a|\beta\rangle_b$. We identify the qubit value S_i at time t_i as "which-way" information. The qubit value for mode a can be determined by a quadrature measurement X_B of the mode b, and the interference for system a created by interacting locally according to $U_A(t_2)$ for a specific time t_2. Similarly, one may apply $U_B(t_2)$ for b. The loss of which-way information is identified by fringes in the distributions of the orthogonal quadrature P_A for a. However, we conclude there is no paradox involving macroscopic retrocausality since the fringes are only distinguished at the level of $\hbar$. The results can be viewed consistently with weak macroscopic realism (wMR). Nonetheless, in Sec. VI we show that at the *microscopic* level of $\hbar$, EPR-type paradoxes can be constructed (similar to those discussed in [33,38]), based on the fringe patterns.

We turn to macroscopic paradoxes, in Sec. IV, by presenting tests based on a delayed-choice Leggett-Garg proposal where it is only necessary to measure macroscopic qubit values S_i. We show violation of a Leggett-Garg inequality, where one measures S_i at three times t_i ($t_3 > t_2 > t_1$). The violation reveals failure of the joint assumptions of *weak macroscopic realism* (wMR) and *noninvasive measurability* (called *macrorealism*). Noninvasive measurability asserts that one can determine the value S_i for the system satisfying wMR, in a way that does not affect the future S_j ($j > i$). In the present proposal, the measurement of S_i ($i = 1, 2$) of a is justified to be noninvasive because it is performed on the spacelike-separated system b and, furthermore, the choice of which measurement (S_1 or S_2) to make is delayed, until after t_3. A natural interpretation is that the measurement of S_2 (or S_1) disturbs the dynamics to affect the result for λ_3, therefore violating macrorealism. Since there is a delayed choice, this suggests macroscopic retrocausality.

In Sec. V, we propose a Chaves-Lemos-Pienaar delayed-choice experiment that applies to macroscopic qubits based on the coherent states $|\alpha\rangle$ and $|-\alpha\rangle$ (cat states) [27]. This involves identification of the appropriate unitary interaction U that takes the role of the beam splitter in the MZ interferometer. We thus predict a violation of the dimension witness inequality for cat states, which would imply falsification of all two-dimensional nonretrocausal MR models. This rules out a class of wMR models, implying the need for extra dimensions if consistency with wMR is to be upheld.

To counter conclusions of macroscopic retrocausality, in Sec. IV C we give an interpretation of the violations of the delayed-choice Leggett-Garg inequalities that is consistent with wMR: The apparent macroscopic retrocausality comes about because of the entanglement with the meter system b at the time t_2, and the macroscopic nonlocality associated with the dynamics of the unitary rotations, when such rotations occur for *both* systems after the time t_2. Using phase-space depictions of $P(X_A, X_B)$, we identify extra dimensions not present in the two-dimensional nonretrocausal models. We show that the violation of the Leggett-Garg inequalities certifies a failure of *deterministic macroscopic realism* (dMR), but not wMR (which is a weaker assumption than dMR).

II. MODELS OF MACROSCOPIC REALISM AND OVERVIEW OF CONCLUSIONS

In this section, we give details of the different definitions of macroscopic realism used in this paper and present an overview of the conclusions reached regarding the validity of each, assuming the predictions of quantum mechanics for the proposed experiments are correct.

Macroscopic realism was defined by Leggett and Garg [35] who considered a system $\mathcal{S}$ which has just two macroscopically distinct states available to it. Macroscopic realism asserts that the system actually be in one or other of these states at all times. In their paper, Leggett and Garg introduced a hidden variable λ_M which takes the value $+1$ or -1 depending on which of the two states the system is in. The hidden variable gives the prediction for a measurement M that can be made on the system in order to determine which of the distinct states the system is in at the time t. However, since the states are macroscopically distinct, the states can be distinguished by a measurement M that allows a macroscopic coarse graining. This motivates a more relaxed definition of macroscopic realism which we use in this paper.

Definition 1: Macroscopic realism (MR) asserts that the system $\mathcal{S}$ can be assigned a hidden variable λ_M, the value of which gives the outcome of the coarse-grained measurement M distinguishing between the two states. The definition of MR does not require the system with outcome $+1$ (or -1) be in a *particular* quantum state ψ_+ (ψ_-), nor even necessarily in any *quantum* state.

It is possible to define two types of macroscopic realism, depending on whether the unitary dynamics associated with the choice of measurement setting has taken place. This leads us to first consider deterministic macroscopic realism.

A. Deterministic macroscopic realism (dMR)

The system $\mathcal{S}$ may have available to it two or more sets of macroscopically distinct states. An example is a system which is found to be in one of two macroscopically distinguishable colors: either blue or red. The hidden variable λ_C takes the value $+1$ or -1, respectively, for red or blue. Simultaneously, the system may be found to be always either with a texture that is soft or hard. The hidden variable λ_T can be assigned to describe the outcome of the measurement distinguishing these textures. We consider such a system at the time t, prior to any measurement. Macroscopic realism asserts that both of these hidden variables can be ascribed to the system at time t, simultaneously.

In a Bohm-Bell experiment, measurements of spin are made on two separated particles, or systems [36,39]. For each system, there is the choice to measure one of two different spin components. Let us consider these components to be S_z and S_x, for one of the systems. The eigenstates are denoted $|\uparrow\rangle_z, |\downarrow\rangle_z$ and $|\uparrow\rangle_x, |\downarrow\rangle_x$, respectively. *If* we were to suppose

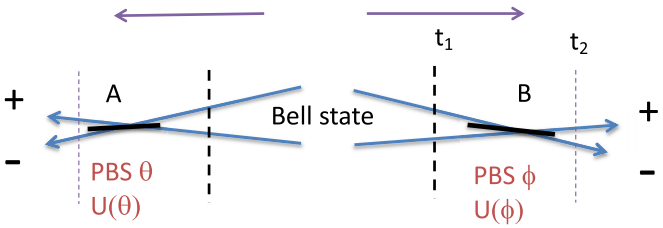

FIG. 2. Sketch of the setup of a Bell-Bohm experiment: the system is prepared in a Bell state where two particles propagate towards detectors at A and B, respectively. The polarizer-beam-splitter (PBS) settings determine the choice of θ and ϕ and hence whether S_x or S_z is measured at each site. Let us suppose that the spin eigenstates represent macroscopically distinct states. Deterministic macroscopic realism (dMR) asserts that the system at time t_1 prior to the unitary rotation U has predetermined values for the outcomes of both S_z and S_x. Weak macroscopic realism (wMR) asserts that the system after the unitary interaction at time t_2 has predetermined outcome for the observation or either $+$ or $-$.

that the two eigenstates represented macroscopically distinct states, then MR would assign hidden variables λ_z and λ_x to determine the outcome of the measurements S_z and S_x, respectively. The possible values of λ_x and λ_z are $+1$ and -1, these representing the Pauli spin outcomes. The definition of deterministic macroscopic realism is that the hidden variables λ_x and λ_z can be assigned to the system, prior to the unitary interaction U_θ (usually realised by a Stern-Gerlach apparatus or polarizing beam splitter) that determines which spin component will be measured (Fig. 2).

Definition 2: Deterministic macroscopic realism (dMR). We consider a pair of macroscopically distinguishable states (labeled θ) that can be distinguished by a measurement M_θ. We allow for multiple pairs θ and associated measurements M_θ. For each θ, MR asserts a hidden variable λ_θ that determines the outcome of a coarse-grained measurement M_θ distinguishing between the two macroscopically distinct states of the system. Deterministic macroscopic realism asserts that these hidden variables describe the system *prior* to the unitary interaction U_θ that determines the measurement setting θ.

Deterministic macroscopic realism can be falsified in a macroscopic Bell-type experiment, *if* the spin states are macroscopically distinct for all relevant measurement settings, θ and ϕ. This allows the assertion of two hidden variables for each system, at the time t_1 in the diagram of Fig. 2. We define $\lambda_\theta^{(A)}$ and $\lambda_{\theta'}^{(A)}$ for system A, and $\lambda_\phi^{(B)}$ and $\lambda_{\phi'}^{(B)}$ for system B, where each λ takes the value $+1$ or -1. As in the original derivations of Bell inequalities [36,40,41], the assumption would imply $|\lambda_\theta^{(A)}\lambda_\phi^{(B)} - \lambda_\theta^{(A)}\lambda_{\phi'}^{(B)} + \lambda_{\theta'}^{(A)}\lambda_\phi^{(B)} + \lambda_{\theta'}^{(A)}\lambda_{\phi'}^{(B)}| \leqslant 2$ and hence a Bell inequality $B \leqslant 2$ follows, where $B = |\langle S_\theta^{(A)} S_\phi^{(B)}\rangle - \langle S_\theta^{(A)} S_{\phi'}^{(B)}\rangle + \langle S_{\theta'}^{(A)} S_\phi^{(B)}\rangle + \langle S_{\theta'}^{(A)} S_{\phi'}^{(B)}\rangle|$. Here, $S_\theta^{(A)}$ and $S_\phi^{(B)}$ are the qubit values for the spin measurements at sites A and B respectively, with the settings θ and ϕ. The dMR model is predicted to be falsified for gedanken experiments involving cat states, in [32,33]. In those treatments, as in this paper, the measurements $\hat{M}_\theta$ distinguish the states $|\alpha\rangle$ and $|-\alpha\rangle$ for all $\alpha \to \infty$, or similar states with macroscopically distinguishable amplitudes in phase space. Violations giving $B > 2\sqrt{2}$ were shown theoretically possible for $\alpha \to \infty$, thus enabling falsification of dMR. Violations of Bell inequalities using measurements with a macroscopic coarse graining were also considered for different states in [42,43].

One may also consider three angle settings: 1, 2, and 3 for each of two systems A and B. The assumption of dMR implies three hidden variables $\lambda_i^{(A)}$ and $\lambda_j^{(B)}$ $(i, j = 1, 2, 3)$ at each site, each taking values $+1$ or -1. This leads to a Bell inequality

$$\langle S_1^{(A)} S_2^{(B)}\rangle + \langle S_2^{(A)} S_3^{(B)}\rangle - \langle S_1^{(A)} S_3^{(B)}\rangle \leqslant 1 \tag{2}$$

similar to that derived in Bell's original paper [36], where all the spin components of each particle were assumed to have definite predetermined values prior to measurement. We may also suppose that the measurements *could* be made on a single system A. Then,

$$B_{lg} \equiv \langle S_1^{(A)} S_2^{(A)}\rangle + \langle S_2^{(A)} S_3^{(A)}\rangle - \langle S_1^{(A)} S_3^{(A)}\rangle \leqslant 1, \tag{3}$$

which is a Leggett-Garg inequality, if the measurements S_i are made at different times and can be made noninvasively [35].

In this paper, we consider three gedanken experiments involving cat states and delayed choice. For the second of those, the apparent retrocausality manifests as a violation of inequalities (2) and (3). We will show that this violation, while suggestive of a macroscopic retrocausal effect, in fact indicates violation of dMR, where the λ_M distinguishes between states $|\alpha\rangle$ and $|-\alpha\rangle$ $(\alpha \to \infty)$.

B. Weak macroscopic realism (wMR)

Since dMR can be falsified, this motivates testing of a weaker form of MR (Fig. 1). In all of the examples using cat states and indeed in the Bell example of Fig. 2, the choice of measurement setting involves a unitary interaction U which takes place over a time interval.

In defining weak macroscopic realism, one considers the definition of MR at a single time t, where the system has been prepared *after* the unitary interaction. In the Bell experiment, the polarizer acts to prepare the system with respect to the pointer basis, so that a photon detection determines the outcomes. The outcomes $+1$ and -1 correspond to a detection at a location $+$ or at a location $-$, respectively (Fig. 2). The system is initially prepared at time t_1 in

$$|\psi_{\rm Bell}\rangle = \frac{1}{\sqrt{2}}\{|\uparrow\rangle_z|\downarrow\rangle_z - |\downarrow\rangle_z|\uparrow\rangle_z\}. \tag{4}$$

If the polarizers are set at angle 0, then this represents the pointer basis and weak macroscopic realism would assert the hidden variables $\lambda_z^{(A)}$ and $\lambda_z^{(B)}$ for the final photon detection at the pointer positions $+$ or $-$. There is *no* assumption that the values for $\hat{S}_x$ are determined, however.

If a further unitary rotation is to take place, so that the spin-x component is measured at systems A and B, then after the unitary rotation at the time t_2, one considers the system to be described by the state

$$|\psi_{\rm Bell}\rangle = \frac{1}{\sqrt{2}}\{|\uparrow\rangle_x|\downarrow\rangle_x - |\downarrow\rangle_x|\uparrow\rangle_x\} \tag{5}$$

in the new basis. Weak macroscopic realism asserts the system to be in a state with a well-defined hidden variable λ_x for the

outcome of S_x at the time t_2, but *not* (necessarily) at the time t_1.

Definition 3: Weak macroscopic realism (wMR). Consider a system prepared in a superposition of pointer states at a time t (after the selection of the measurement setting θ), e.g.,

$$|x\rangle + |-x\rangle, \tag{6}$$

where $|x\rangle$ and $|-x\rangle$ are macroscopically distinct states corresponding to macroscopically distinct positions (locations) of a photon, or of a macroscopic object. Weak macroscopic realism asserts that the system can be described by a hidden variable λ_M, which takes the value $+1$ or -1 to determine that the outcome of the pointer measurement M will be either x or $-x$, respectively. We note that as the distinction between x and $-x$ is macroscopic, the hidden variable need not determine the precise value of x, i.e., it is coarse grained. In this paper, we propose three delayed-choice macroscopic experiments and show that all three can be explained consistently with wMR.

C. Two-dimensional wMR models

The values for the hidden variables in the tests of wMR and dMR that we will consider are dichotomic ($+1$ or -1). At the times examined in the tests, quantum mechanics predicts the systems to be in superposition of just two states, $|\alpha\rangle$ and $|-\alpha\rangle$. We find in this paper that it is possible to negate wMR, if restricted to a two-dimensional model.

If one assumes a *two-dimensional classical nonretrocausal model*, then the system is described by the hidden variable λ_M as above, taking values $+1$ and -1. With a restriction on the dimensionality, constraints exist of the correlations [27]. For a single system A, consider a setup with settings given by θ at a time t_p and ϕ at a later time t_m. It has been shown that all two-dimensional models that are not retrocausal satisfy a dimension witness (DW) inequality [44–47] involving the expectation value of an observable S_ϕ at time t_m, given the previous setting of θ [27]. The Wheeler-CLP experiment gives a negation of such models. In this paper, we apply this result to propose a macroscopic version of the CLP experiment, where a hidden variable λ_M refers to macroscopically distinct states, and the two-dimensional nonretrocausal model is therefore also a two-dimensional wMR model.

Definition 4: Two-dimensional wMR models. We consider a two-dimensional classical model, as in the Definition 1 of macroscopic realism (MR). For a single system A, we consider a setup with settings given by θ at a time t_p and ϕ at a later time t_m. Supposing the system at each time is given by two states so that wMR applies at the times t_p and t_m, then two hidden variables λ_p and λ_m can be assigned to describe the outcome of the measurement M at those times. With the restriction of a two-dimensional model, this leads to the same dimension witness (DW) inequality

$$I_{\rm DW} = |E(\theta,\phi) + E(\theta,\phi') + E(\theta',\phi) - E(\theta',\phi') - E(\theta'',\phi)| \leqslant 3 \tag{7}$$

derived for qubits originally in the microscopic regime [27]. Here $E(\theta,\phi) = \langle S_\phi\rangle_\theta$ is the expectation value of S_ϕ at time t_m, given the previous setting of θ.

We show in this paper that the inequality (7) is violated for dynamical cat states and therefore that all two-dimensional wMR models can be negated for this system (Fig. 1). In fact, an analysis of the dynamics shows that at intermediate times between t_p and t_m, the system is not a simple superposition of just two coherent states. Moreover, we will compare with a system evolving from a classical mixture of the two coherent states, which does not violate the DW inequality. The dynamics in the multi-dimensional phase space shows the emergence of the quantum correlations over the duration of the unitary dynamics occurring between times t_p and t_m.

D. Quantum macroscopic realism (QMR) models

As explained above, the original definition of macroscopic realism as quoted by Leggett and Garg considers a system with two macroscopically distinct states available to it, and then proposes that the system be in one or other of those two states.

Definition 5: Quantum macroscopic realism (QMR). If it is assumed that the two states specified in the MR definition are well defined as *quantum* states (ρ_+ and ρ_-), then this is a further restriction imposed on the definition of MR. We call such a refined definition of macroscopic realism "*quantum macroscopic realism (QMR)*", because the states associated with the hidden variable λ_M taking a value $+1$ or -1 are then the states ρ_+ or ρ_-, respectively. All QMR models satisfy weak macroscopic realism for the appropriate pointer measurement.

It is possible to negate QMR models, which were also considered in [38]. Rigorous signatures of a Schrödinger-cat paradox will exclude the possibility of a system being in one or other of two macroscopically distinguishable quantum states, though often specific quantum states are assumed, as in [34]. The observation of a strict form of macroscopic quantum coherence will also imply negation of QMR. If it is possible to exclude that the system is in a mixture of two quantum states ρ_+ and ρ_-, where the only condition on ρ_+ and ρ_- is that these states give predictions $+1$ and -1 for the measurement M, then the QMR models are directly negated.

In Sec. VI, we illustrate how the QMR models can be negated for the cat states considered in this paper. If one begins with the premise of local realism, or else if one assumes weak macroscopic realism, then all QMR models can be negated.

E. Conclusions

In this paper, we consider three gedanken experiments involving cat states and delayed choice. For the second of those, we confirm violation of deterministic macroscopic realism (dMR). All three gedanken experiments can be viewed consistently with weak macroscopic realism. However, the third delayed-choice experiment violates the DW inequality (7), thus negating two-dimensional wMR nonretrocausal models. In all these experiments, "macroscopic" implies a distinction between amplitudes α and $-\alpha$ of a cat state, for $\alpha \to \infty$. For some states, we are able to show inconsistency between weak macroscopic realism (wMR) and quantum macroscopic realism (QMR), thus ruling out the class of wMR models satisfying QMR. The different models of macroscopic realism and the relationship between them are depicted in Fig. 1.

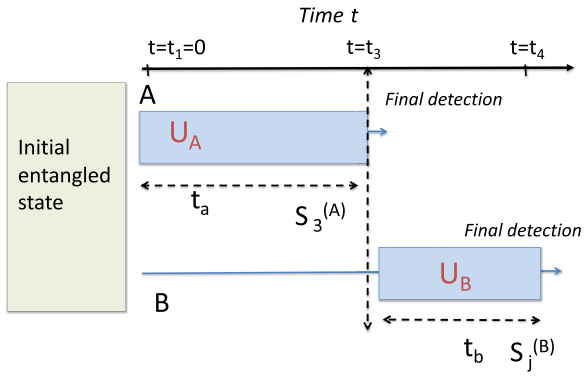

FIG. 3. Sketch of the setup for the quantum eraser test. The system is prepared in the two-mode entangled cat state $|\psi_{\rm Bell}(t_1)\rangle$ at the time $t_1 = 0$, with the modes spatially separated. The values of $S_1^{(A)}$ and $S_1^{(B)}$ at time t_1 are anticorrelated. Independent local unitary interactions U_A and U_B take place at sites A and B, respectively, with time settings t_a and t_b. The time at A is selected as $t_a = t_3 = \pi/2\Omega$. The final detection enables measurement of $S_3^{(A)}$, with an equal probability for outcomes $S_3^{(A)} = 1$ or -1. At B, one selects either $t_b = t_1 = 0$ or $t_b = t_3 = \pi/2\Omega$, the final detection enabling measurement of $S_1^{(B)}$ or $S_3^{(B)}$. The outcomes of $S_1^{(B)}$and $S_3^{(B)}$ are anticorrelated with the outcomes of $S_1^{(A)}$ and $S_3^{(A)}$, respectively, if measured. The choice of the interaction time at B is delayed until after the final detection at A, at time t_3. The value of $S_3^{(A)}$ can be inferred by measuring $S_B^{(3)}$, in which case it is known which state the system A was in at the past time t_3. The fringes in P_A for system A then vanish, conditional on the result at B. On the other hand, if the value of $S_1^{(B)}$ is measured, then $S_1^{(A)}$ is known but there is no information about $S_3^{(A)}$ and fringes are present. We argue that the results are not inconsistent with the validity of weak macroscopic realism (wMR): wMR asserts that the system A at time t_3 *is* in a state with a definite value ($+1$ or -1) of $S_3^{(A)}$ and that this value is merely elucidated by the later measurement of $S_3^{(B)}$. There is a paradox, however, because one may show that the system A at the time t_3 *cannot* be regarded as being in any quantum state with a definite value for $S_3^{(A)}$.

III. DELAYED-CHOICE QUANTUM ERASER WITH ENTANGLED CAT STATES

A. Setup

We begin by presenting an analog of the delayed-choice quantum eraser experiment for cat states (Fig. 3). The overall system is prepared at time $t_1 = 0$ in the entangled cat Bell state [48]

$$|\psi_{\rm Bell}(t_1)\rangle = \mathcal{N}(|\alpha\rangle|-\beta\rangle - |-\alpha\rangle|\beta\rangle), \tag{8}$$

where $|\alpha\rangle$ and $|\beta\rangle$ are coherent states for single-mode systems A and B. We take α and β to be real, positive, and large. Here, $\mathcal{N} = \frac{1}{\sqrt{2}}\{1 - \exp(-2|\alpha|^2 - 2|\beta|^2)\}^{-1/2}$ is the normalization constant.

For each system, one may measure the field quadrature phase amplitudes $\hat{X}_A = \frac{1}{\sqrt{2}}(\hat{a} + \hat{a}^\dagger)$, $\hat{P}_A = \frac{1}{i\sqrt{2}}(\hat{a} - \hat{a}^\dagger)$, $\hat{X}_B = \frac{1}{\sqrt{2}}(\hat{b} + \hat{b}^\dagger)$, and $\hat{P}_B = \frac{1}{i\sqrt{2}}(\hat{b} - \hat{b}^\dagger)$, which are defined in a rotating frame, with units so that $\hbar = 1$ [34]. The boson destruction operators for modes A and B are denoted by $\hat{a}$ and $\hat{b}$, respectively. The outcome of the measurement $\hat{X}_A$ distinguishes between the states $|\alpha\rangle$ and $|-\alpha\rangle$, and similarly $\hat{X}_B$ distinguishes between the states $|\beta\rangle$ and $|-\beta\rangle$. Dropping the operator "hats" where the meaning is clear, we define the outcome of a macroscopic qubit measurement $S^{(A)}$ on system a to be $S^{(A)} = +1$ if $X_A > 0$, and -1 otherwise. Similarly, the outcome of a macroscopic qubit measurement $S^{(B)}$ on system b is $S^{(B)} = +1$ if $X_B > 0$, and -1 otherwise. S is identified as the spin of the system, i.e., the qubit value.

The coherent states of A and B become orthogonal in the limit of large α and β, in which case the superposition (8) maps onto the two-qubit Bell state

$$|\psi_{\rm Bell}\rangle = \frac{1}{\sqrt{2}}(|+\rangle_a|-\rangle_b - |-\rangle_a|+\rangle_b). \tag{9}$$

At time t_1, the outcomes for $S^{(A)}$ and $S^{(B)}$ are anticorrelated. Therefore, one may infer the outcome for $S^{(A)}$ noninvasively by measuring X_B, and hence $S^{(B)}$.

We present an analogy with the delayed-choice quantum eraser based on the photonic versions of the state (9). In the photonic version, the next step is that the photon of system A propagates through two slits, or else through a 50/50 beam splitter ($\rm BS_1$) with two equally probable output paths as in a Mach-Zehnder (MZ) interferometer. If a single photon is incident on $\rm BS_1$, this creates a superposition, e.g., for mode A, the state $|+\rangle_a$ is transformed to

$$|\psi\rangle_{a,2} = \frac{1}{\sqrt{2}}(|+\rangle_{a,2} + i|-\rangle_{a,2}), \tag{10}$$

where $|+\rangle_{a,2}$ and $|-\rangle_{a,2}$ refer to the photon in paths designated $+$ or $-$ of the MZ interferometer. In the original quantum eraser, the measurement of which-way information is made by measuring whether the system is $+$ or $-$. This is done by recombining the paths using a second beam splitter ($\rm BS_2$), which is set to be fully transmitting so that the paths are not mixed. An alternative choice is that $\rm BS_2$ is similar to $\rm BS_1$ with a 50% transmittivity, which restores the state $|+\rangle$, the photon appearing only at one of the output paths, indicating interference.

In the cat-state gedanken experiment (Fig. 3), the superposition (10) is achieved by a unitary interaction $U(t)$ for a particular choice $t = t_3$. After preparation at the time t_1, the systems A and B evolve independently according to the local unitary transformations $U_A(t_a)$ and $U_B(t_b)$, defined by

$$U_A(t_a) = e^{-iH_{\rm NL}^{(A)}t_a/\hbar}, \quad U_B(t_b) = e^{-iH_{\rm NL}^{(B)}t_b/\hbar}, \tag{11}$$

where

$$H_{\rm NL}^{(A)} = \Omega\hat{n}_a^k, \quad H_{\rm NL}^{(B)} = \Omega\hat{n}_b^k. \tag{12}$$

Here, t_a and t_b are the times of evolution at each site, k is a positive integer, $\hat{n}_a = \hat{a}^\dagger\hat{a}$ and $\hat{n}_b = \hat{b}^\dagger\hat{b}$, and Ω is a constant. We take $k = 2$; or else $k > 2$ and k is even. As the systems evolve, the spin for each can be measured at a given time. We denote the value of spin $S^{(A)}$ after an interaction time $t_a = t_i$ to be $S_i^{(A)}$, and the value of the spin $S^{(B)}$ after the interaction time $t_b = t_j$ to be $S_j^{(B)}$. The dynamics of the unitary evolution (11) is well known [34,49,50]. If the system A is prepared in a coherent state $|\alpha\rangle$, then after a time $t_a = t_3 = \pi/2\Omega$, the state of the system A is [31–33]

$$U_{\pi/4}^{(A)}|\alpha\rangle = e^{-i\pi/4}\{\cos\pi/4|\alpha\rangle + i\,\sin\pi/4|-\alpha\rangle\}, \tag{13}$$

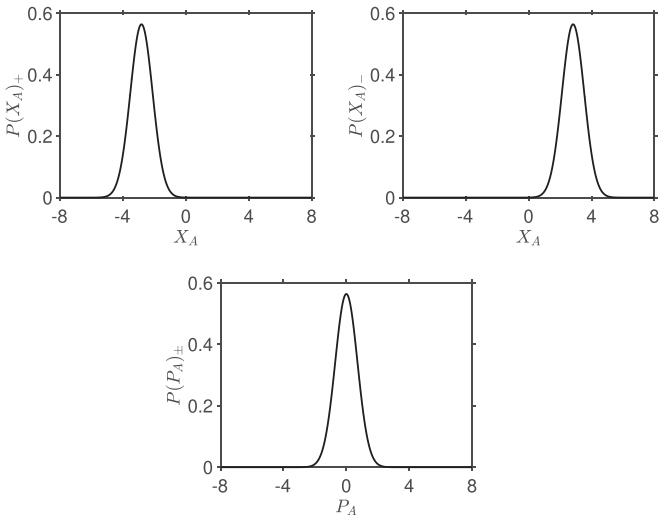

FIG. 4. Plots of $P(X_A)_\pm$ and $P(P_A)_\pm$ for the system A at time t_3, when which-way information is present. The $P(X_A)_\pm$ and $P(P_A)_\pm$ are distributions conditioned on the outcome $\pm$ for X_B at B. The $P(P_A)_+$ and $P(P_A)_-$ are identical and show no fringes. Here, $\alpha = \beta = 2$.

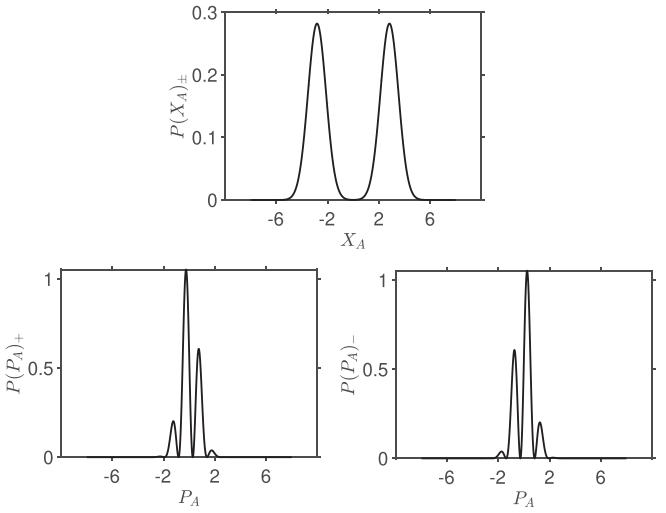

FIG. 5. Plots of $P(X_A)_\pm$ and $P(P_A)_\pm$ of the system A at time t_2, where the outcome for $S_4^{(B)} = S_A^{(1)}$ is (lower left) $+1$, and (lower right) -1. The which-way information is lost, and the system A is in the superposition (16). Here, $\alpha = \beta = 2$.

where $U_{\pi/4}^{(A)} = U_A(\pi/2\Omega)$. A similar transformation $U_{\pi/4}^{(B)}$ is defined at B for $t_b = t_3 = \pi/2\Omega$. We note the state (13) maps onto (10). The generation of the superposition (13) using $k = 2$ has been reported in [49,50]. The system A in the superposition (13) exhibits interference fringes in the distribution $P(P_A)$ for $\hat{P}_A$ [34].

If one evolves for a time of $t_3 = \pi/2\Omega$ at both sites, then the final state is

$$|\psi_{\rm Bell}(t_3)\rangle = U_{\pi/4}^{(A)} U_{\pi/4}^{(B)} |\psi_{\rm Bell}(t_1)\rangle = \mathcal{N} e^{-i\pi/2}(|\alpha\rangle|-\beta\rangle - |-\alpha\rangle|\beta\rangle), \quad (14)$$

which is a Bell state. At the time t_3, the spin $S_3^{(A)}$ of system A can be inferred by measuring $S_3^{(B)}$, which is anticorrelated with the spin $S_3^{(A)}$ at A. This gives the which-way information of system A at time t_3, analogous to measuring through which slit or path the photon went through in the original quantum eraser setups. Only the absolute interaction times t_a and t_b at each site are relevant to the correlation, however, and it is hence possible to *delay* interaction at B until a time t_4, after the system at A has already interacted.

With this method of measurement of $S_3^{(A)}$, the system A has not been directly measured. One can thus make a measurement of $\hat{P}_A$ at the time t_3. The system (being coupled to B) can be detected as being in one or other state, φ_+ or φ_-, giving $+$ or $-$ outcomes for $S_3^{(A)}$. Which-way information is present and, consistent with that, the distribution $P(P_A)$ shows no fringes. This is seen in Fig. 4, where we plot the conditional distributions $P(X_A)_\pm$ and $P(P_A)_\pm$ given the outcome $\pm$ for X_B at B, as evaluated from the joint distributions $P(X_A, X_B)$ and $P(P_A, X_B)$. The distribution $P(P_A)_\pm$ for an outcome of the measurement $\hat{P}_A$ is a Gaussian centered at 0 with no fringes present, consistent with that of the coherent state $|\pm\alpha\rangle$ [34].

On the other hand, one may take $t_a = t_3$ and $t_b = 0$, so that there is no local unitary interaction at B. Alternatively, one may evolve both sites according to $t_a = t_b = t_3$, and then perform a local unitary transformation $U_B(t_2)^{-1} = (U_{\pi/4}^{(B)})^{-1}$ at B, to transform the system B "back" to the initial state of B at time t_1. Which-way information about A at t_3 is then absent. The state of the combined systems at this time $t_4 > t_3$ is

$$|\psi(t_4)\rangle = \mathcal{N}\{U_{\pi/4}^{(A)}|\alpha\rangle|-\beta\rangle - U_{\pi/4}^{(A)}|-\alpha\rangle|\beta\rangle\}. \quad (15)$$

If the final stage of the spin measurement B is made at time t_4, the result will give either $S^{(B)}(t_4) = 1$ or -1. From the anticorrelation of (8), $S^{(B)}(t_4)$ is interpreted as a measurement of the initial value of $-S_1^{(A)}$, and hence knowledge of that state of system A at that time t_1. If the outcome of $S^{(B)}(t_4)$ is ∓ 1, then, assuming the limit where $|-\beta\rangle$ and $|\beta\rangle$ are orthogonal states (i.e., large β), the system A is projected into the superposition state

$$U_{\pi/4}|\pm\alpha\rangle = e^{-i\pi/4}\{\cos\pi/4|\pm\alpha\rangle + i\,\sin\pi/4|\mp\alpha\rangle\}. \quad (16)$$

This is the state of the local system A at time t_2 [see Eq. (13)], conditioned on the initial state of A at time t_1 being $|\pm\alpha\rangle$. Thus, if one measures $P(P_A)$ conditional on the result of $-S^{(B)}(t_4) = S_1^{(A)}$, the fringes are recovered. We find

$$P(P_A)_\pm = \frac{e^{-P_A^2}}{\sqrt{\pi}}\{1 \mp \sin(2\sqrt{2}P_A|\alpha|)\}, \quad (17)$$

where $P(P_A)_+$ and $P(P_A)_-$ are the distributions for P_A conditional on the result $+1$ or -1 for $S_1^{(A)}$, respectively. The distributions (Fig. 5) show fringes, indicative of the system A at time t_3 being in the superposition (16), and indicative of the loss of which-way information.

The accurate calculation of the conditional probabilities $P(P_A)_\pm$, without the simplistic assumption of a projection into a definite coherent state at A on measurement at B, gives

$$P(P_A)_\pm = \frac{2\mathcal{N}^2 e^{-P_A^2}}{\sqrt{\pi}}\{1 - e^{-2|\beta|^2}\cos(2\sqrt{2}P_A|\alpha|) \mp \sin(2\sqrt{2}P_A|\alpha|)\mathrm{erf}(\sqrt{2}|\beta|\}, \quad (18)$$

where erf is the error function (refer Appendix 1). The plots are indistinguishable from those of the approximate result for $\beta > 1$, the limit $\beta \to \infty$ being the limit of an ideal measurement. The calculations in Figs. 4 and 5 are based on evaluation of the joint distribution $P(P_A, X_B)$ (refer to [32]).

B. Interpretation in terms of wMR

As summarized in the Introduction, the delayed choice experiment has been interpreted as suggesting retrocausality. The decision to observe either the particlelike behavior (which-way information) or the wavelike behavior (fringes) of system A is made at the later time t_4 (at B). This appears to retrospectively change the system A at time t_3 from being in "one or other state" (φ_1 *or* φ_2; $|\alpha\rangle$ or $|-\alpha\rangle$) to being "in both states" [since the observation of fringes in $P(P_A)$ is often interpreted to suggest the system A was in "both states", $|\alpha\rangle$ and $|-\alpha\rangle$]. As explained in [27], there is in fact no requirement to assume retrocausality for the MZ delayed-choice experiment. The experiment described for cat states maps onto the qubit experiment for large α, β, and gives a similar conclusion for the macroscopic qubits.

The macroscopic version of the quantum eraser is informative because, with the introduction of the macroscopic hidden variable λ_M, there is a separation of the macroscopic from the microscopic behaviour. According to the premise of weak macroscopic realism (wMR), at the time t_3 the system (13) may be regarded as being in one or other of two macroscopically distinguishable states (φ_+ and φ_-) which have a definite value $+1$ or -1 for the outcome $S_3^{(A)}$, should that measurement be performed. Here, there is no attempt to define the *quantum* state associated with that predetermination, so that predictions for other more microscopic measurements (and hence other hidden variables that determine those predictions) are not relevant. While it might be tempting to identify the states φ_+ and φ_- as being $|\alpha\rangle$ and $|-\alpha\rangle$, this would be a full microscopic identification of the states in quantum terms. The states φ_+ and φ_- are not specified to this precision, corresponding to distinct values of the macroscopic observable $S_3^{(A)}$ only. In fact, we see there is *no negation of wMR* because the fringes are only evident at the microscopic level of $\hbar$ (here $\hbar \sim 1$). The gedanken experiment is consistent with wMR. In that sense, the system always displays a particlelike behavior.

The determination of the value of $S_3^{(A)}$ gives the "which-way" information in the quantum eraser experiment. If one is able to design an appropriate macroscopic observable (similar to $S_3^{(A)}$) for the two-slit and MZ scenarios, then the assumption of wMR is analogous to the interpretation that the particle goes through one slit or the other in the double-slit experiment, or goes through one path or the other, in the MZ interferometer. This assumption, however, does not specify the system to be in either state $|-\alpha\rangle_{a,2}$ or $|\alpha\rangle_{a,2}$ [refer to Eq. (10)]. The assumption of wMR if applied to the double-slit experiment would be that the particle has a position constraining it to go through a definite slit, even when fringes are observed (provided the slit does not restrict the position to of order $\hbar$ or less). In relation to the definition of wMR, the predictions for other more precise measurements of order $\hbar$ are not relevant.

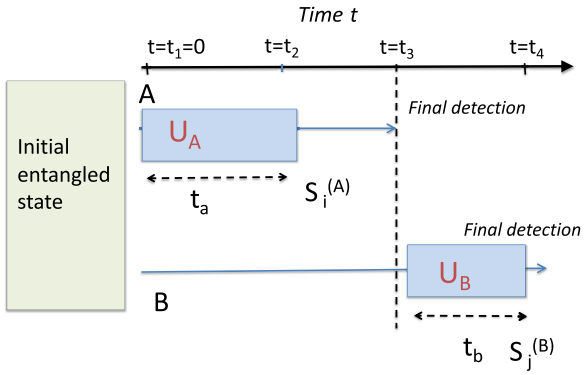

FIG. 6. Sketch of the setup for the delayed-choice Leggett-Garg test. The system is prepared in the two-mode entangled cat state $|\psi_{\rm Bell}(t_1)\rangle$ at the time $t_1 = 0$, with the modes spatially separated. Independent local unitary interactions U_A and U_B take place at sites A and B, respectively, with time settings t_a and t_b. The times at A are selected as either $t_a = t_2 = \pi/4\Omega$ or $t_a = t_3 = \pi/2\Omega$ and the final detection enables measurement of $S_2^{(A)}$ or $S_3^{(A)}$ respectively. At B, one selects either $t_b = t_1 = 0$ or $t_b = t_2 = \pi/4\Omega$, the final detection enabling measurement of $S_1^{(B)}$ or $S_2^{(B)}$. The outcomes of $S_1^{(B)}$and $S_2^{(B)}$ are anticorrelated with the outcomes of $S_1^{(A)}$ and $S_2^{(A)}$, respectively, if measured. In the delayed-choice experiment, the interaction at B is delayed until after the final detection at A, at time t_3. Hence, the measurement of $S_1^{(B)}$ (or $S_2^{(B)}$) allows inference of the past value of $S_1^{(A)}$ (or $S_2^{(A)}$). The results indicate a violation of a Leggett-Garg inequality, which we show implies failure of deterministic macroscopic realism (dMR) but can be explained consistently with weak macroscopic realism (wMR).

The interpretation based on wMR suggests a lack of completeness of the description at the microscopic level. This can be clarified further. Indeed, if wMR holds, then it is possible to show that EPR-type paradoxes exist at the microscopic level. The EPR-type arguments indicate an *incompleteness* of a quantum state description if compatible with wMR [33], and are discussed in Sec. VI.

IV. DELAYED-CHOICE LEGGETT-GARG TEST OF MACROREALISM

In this section, we consider the delayed-choice experiment in the form of a Leggett-Garg test of macrorealism using entangled cat states. The advantage of the Leggett-Garg test is that all relevant measurements are macroscopic, distinguishing between the two macroscopically distinct coherent states. This contrasts with the quantum eraser proposal, where the paradoxical effects are inferred by the measurement of finely resolved fringes.

A. Setup

At time t_1, the system is prepared in the entangled cat state $|\psi_{\rm Bell}(t_1)\rangle$ of Eq. (8). The modes are spatially separated systems at sites A and B, and dynamically evolve according to the unitary interactions (11) where $k = 4$. We consider three times $t_1 = 0$, $t_2 = \pi/4\Omega$, and $t_3 = \pi/2\Omega$ (Fig. 6). If the system at A were prepared in a coherent state $|\alpha\rangle$, then at the later time $t_a = t_2 = \pi/4\Omega$, the state of the system A at time t_2

is in the asymmetric superposition [31–33]

$$U^{(A)}_{\pi/8}|\alpha\rangle = e^{-i\pi/8}\{\cos\pi/8|\alpha\rangle + i\,\sin\pi/8|-\alpha\rangle\}, \quad (19)$$

where $U^{(A)}_{\pi/8} = U_A(\pi/4\Omega)$. A similar transformation $U^{(B)}_{\pi/8}$ is defined at B for $t_b = t_2 = \pi/4\Omega$. If one evolves for a time of $t_2 = \pi/4\Omega$ at both sites, then the final state is

$$\begin{aligned}|\psi_{\rm Bell}(t_2)\rangle &= U^{(A)}_{\pi/8}U^{(B)}_{\pi/8}|\psi_{\rm Bell}(t_1)\rangle \\ &= \mathcal{N}e^{-i\pi/4}(|\alpha\rangle|-\beta\rangle - |-\alpha\rangle|\beta\rangle). \end{aligned} \quad (20)$$

The values of the macroscopic spins after the interaction time t_2 at each site are denoted $S^{(A)}_2$ and $S^{(B)}_2$. The spin $S^{(A)}_2$ of system A can be inferred by measuring $S^{(B)}_2$ which is anticorrelated with the spin at A.

On the other hand, one may choose to evolve at A for a time $t_a = t_2 = \pi/4\Omega$, but *not* at the site B, so that $t_b = 0$. The state after these interactions is

$$|\psi(t_2,t_1)\rangle = \mathcal{N}\big\{U^{(A)}_{\pi/8}|\alpha\rangle|-\beta\rangle - U^{(A)}_{\pi/8}|-\alpha\rangle|\beta\rangle\big\}. \quad (21)$$

If the final readout stage of the spin measurement at B is made at time t_4 (Fig. 6), the result will give a value $S^{(B)}(t_4) \equiv S^{(B)}_1 = \pm 1$. From $|\psi_{\rm Bell}(t_1)\rangle$ [Eq. (8)], the value of $S^{(B)}(t_4)$ is anticorrelated with the initial value of $S^{(A)}_1$, if we had chosen $t_a = t_1 = 0$. Therefore, the measurement at B is interpreted as a measurement of $S^{(A)}_1$. If the outcome of $S^{(B)}(t_4)$ is ∓ 1 then (assuming $|\beta\rangle$ and $|-\beta\rangle$ are orthogonal) from (15) we see that the system A is reduced to the superposition state

$$U_{\pi/8}|\pm\alpha\rangle = e^{-i\pi/8}\{\cos\pi/8|\pm\alpha\rangle + i\,\sin\pi/8|\mp\alpha\rangle\}. \quad (22)$$

This is the state of the local system A at time t_2 [see Eq. (13)], conditioned on the initial state of A at time t_1 being $|\pm\alpha\rangle$. The value of $S^{(A)}_2$ can be measured directly at A. This combination of interactions therefore allows measurement of both $S^{(A)}_2$ and $S^{(A)}_1$.

Alternatively, we may evolve the system A for a time $t_a = t_3 = \pi/2\Omega$, while not evolving at B ($t_b = t_1 = 0$). This gives

$$|\psi(t_3,t_1)\rangle = \mathcal{N}\big\{U^{(A)}_{\pi/4}|\alpha\rangle|-\beta\rangle - U^{(A)}_{\pi/4}|-\alpha\rangle|\beta\rangle\big\}, \quad (23)$$

where $U_{\pi/4}|\pm\alpha\rangle$ is given by Eq. (13). The spin $S^{(A)}_3$ can be measured directly at A. Measurement of $S^{(B)}(t_4) \equiv S^{(B)}_1$ at B gives the inferred result for the measurement $S^{(A)}_1$. This allows measurement of both $S^{(A)}_3$ and $S^{(A)}_1$.

Alternatively, one may select $t_b = t_2 = \pi/4\Omega$ at B. According to (20), the measurement at B then allows measurement of $S^{(A)}_2$. If one evolves at A for a time $t_a = t_3 = \pi/2\Omega$, then this combination of interactions allows measurement of both $S^{(A)}_2$ and $S^{(A)}_3$.

The setup (Fig. 6) allows for a delayed choice of the measurement of either $S^{(A)}_1$ or $S^{(A)}_2$, by delaying the choice at B to measure either $S^{(B)}_1$ or $S^{(B)}_2$. This amounts to a delay in the choice to interact the system B for a time $t_b = 0$, or else to interact system B for a time $t_b = t_2$. This choice can be delayed until a time well after the time t_3, and well after the final detection (given by the measurement and readout of X_A) takes place at A.

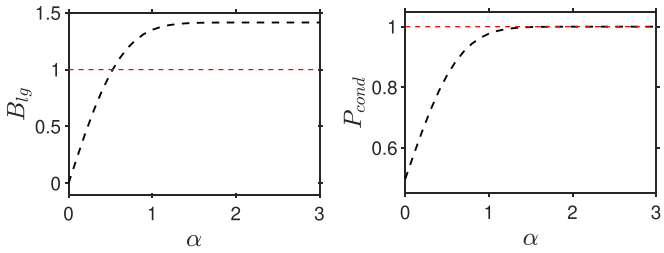

FIG. 7. Violation of the Leggett-Garg inequality (24). We plot $B_{\rm LG} = -\{\langle S^{(B)}_1 S^{(A)}_2\rangle - \langle S^{(B)}_1 S^{(A)}_3\rangle + \langle S^{(B)}_2 S^{(A)}_3\rangle\}$ versus α for the state $|\psi_{\rm Bell}(t_1)\rangle$ (8), with $\beta = 2$. Violation is obtained when $B_{\rm LG} > 1$. The verification of $\langle S^{(A)}_i S^{(A)}_j\rangle = -\langle S^{(B)}_i S^{(A)}_j\rangle$ for $i = 1, 2$ is given by the conditional distribution $P_{\rm cond}$ defined as $P_{\rm cond} = P(S^{(A)}_i = 1|S^{(B)}_i = -1)$ as shown.

B. Leggett-Garg inequality and violations

We now summarize the Leggett-Garg test of macrorealism for this system [33]. The definition of macrorealism involves two assumptions: macroscopic realism and noninvasive measurability (NIM). For our purposes, we take the definition of macroscopic realism to be that of weak macroscopic realism (wMR) defined in Sec. II: This asserts that the system given by (1) is in a state with a definite prediction for the macroscopic spin $S^{(A)}$, $+1$ or -1. The system can then be assigned the hidden variable λ, the value of λ being $+1$ or -1, which determines the result of the measurement $S^{(A)}$ should it be performed. Macrorealism also assumes NIM, that the value of λ can be measured with negligible effect on the subsequent macroscopic dynamics of the system.

For measurements of spin $S^{(A)}_j$ made on a single system A at consecutive times $t_1 < t_2 < t_3$, macrorealism implies the Leggett-Garg inequality [35,51,52]

$$B_{\rm LG} = \left\langle S^{(A)}_1 S^{(A)}_2\right\rangle + \left\langle S^{(A)}_2 S^{(A)}_3\right\rangle - \left\langle S^{(A)}_1 S^{(A)}_3\right\rangle \leqslant 1. \quad (24)$$

As shown in [31–33], the cat system of Sec. IV A is predicted to violate this inequality (Fig. 7), meaning that macrorealism is falsified. While other Leggett-Garg inequalities have been proposed (e.g., [35,53,54]), this particular inequality is useful where measurements are made on entangled subsystems. The approach we give in this paper uses spatial separation *and* delayed choice to justify noninvasiveness, since the measurements of $S^{(A)}_1$ and $S^{(A)}_2$ are made by inference, after performing a delayed measurement on the spacelike-separated system B. The approach can be applied to other macroscopic superposition states, such as NOON states [55,56] using the local unitary interaction given in [32]. Violations of Leggett-Garg inequalities have been predicted and tested for a range of superposition states (e.g., [57–68]) and alternative procedures exist to justify NIM.

We summarize the measurements enabling a test of the inequality (24), as in Figs. 8 and 9. As we have seen, the value of $S^{(A)}_1$ or $S^{(A)}_2$ of system A can be inferred noninvasively by measurement of the anticorrelated spin $S^{(B)}_1$ or $S^{(B)}_2$. The result for the moment $\langle S^{(A)}_1 S^{(A)}_2\rangle$ is determined by a direct measurement of $S^{(A)}_2$ at time t_2, and an inferred measurement of $S^{(A)}_1$ by measuring $S^{(B)}_1$ at B (Fig. 8, top). The moment $\langle S^{(A)}_1 S^{(A)}_3\rangle$ is measured similarly (Fig. 8, lower).

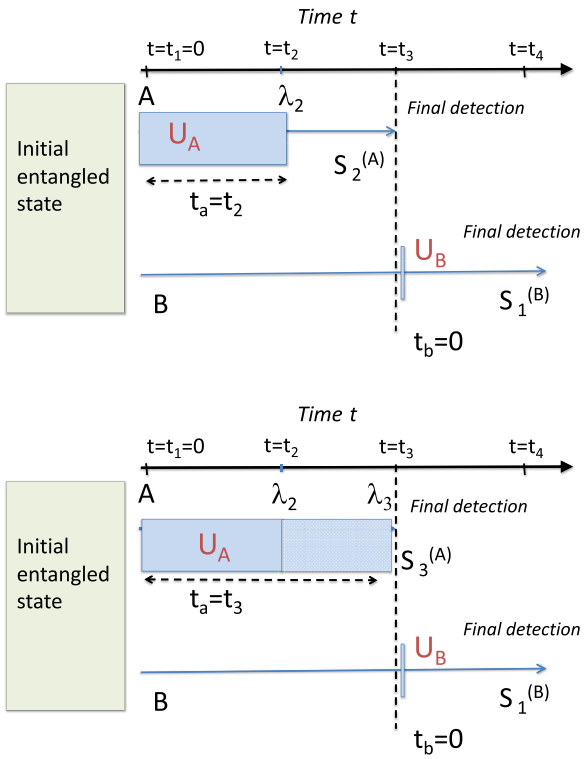

FIG. 8. Sketch of the setup for the delayed-choice Leggett-Garg test. Notation is as for Fig. 6. The top (lower) sketch shows measurement of $\langle S_2^{(A)} S_1^{(B)}\rangle$ ($\langle S_3^{(A)} S_1^{(B)}\rangle$). These measurements give the values of $\langle S_2^{(A)} S_1^{(A)}\rangle$ and $\langle S_3^{(A)} S_1^{(A)}\rangle$, based on the anticorrelation $S_1^{(B)} = -S_1^{(A)}$. For this measurement, there is no unitary interaction (rotation) at B. The predictions for the relevant distributions are given in Fig. 10 (top). The results here are consistent with macrorealism, being indistinguishable from those of the initial nonentangled state $\rho_{\rm mix}$ given by Eq. (26) [compare Fig. 11 (top)].

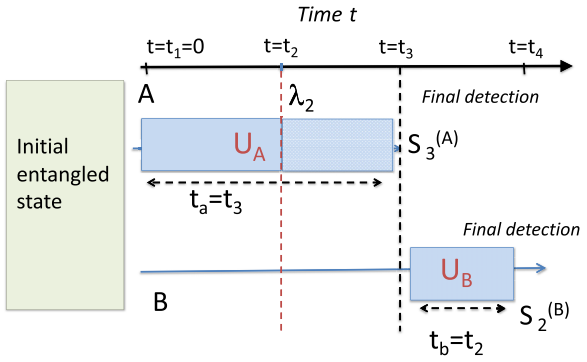

FIG. 9. Sketch of the setup for the Leggett-Garg test. Notation is as for Fig. 6. The sketch depicts measurement of $\langle S_3^{(A)} S_2^{(B)}\rangle$, which (based on the anticorrelation $S_2^{(B)} = -S_2^{(A)}$) gives the value for $\langle S_3^{(A)} S_2^{(A)}\rangle$. The predictions for the relevant distributions are given in Fig. 10 (lower). The results at time t_4 are macroscopically different from those obtained if the state at time t_2 is not entangled [compare Fig. 11 (lower)]. The results are inconsistent with the premise of deterministic macroscopic realism (dMR) and lead to the violation of macrorealism.

The quantum prediction for $\langle S_1^{(A)} S_2^{(A)}\rangle$ is based on the assumption that the measurement of $S_1^{(B)}$ projects the system A into one or other state, $|\alpha\rangle$ or $|-\alpha\rangle$. The prediction is then $\langle S_1^{(A)} S_2^{(A)}\rangle = \cos(\pi/4)$, based on the evolution time of t_2 at A [see Eq. (22)]. The moment $\langle S_1^{(A)} S_3^{(A)}\rangle$ is evaluated similarly, and from Eq. (13) we see the prediction is $\langle S_1^{(A)} S_3^{(A)}\rangle = \cos(\pi/2) = 0$.

For $\langle S_2^{(A)} S_3^{(A)}\rangle$, one would measure $S_2^{(B)}$ to determine the anticorrelated $S_2^{(A)}$, and measure $S_3^{(A)}$ directly at A (Fig. 9). The prediction for $\langle S_2^{(A)} S_3^{(A)}\rangle$ is based on the assumption that the system A is in either $|\alpha\rangle$ or $|-\alpha\rangle$, at time t_2 (or else, that the measurement of $S_2^{(B)}$ projects A to one of these states). The subsequent evolution for a time $\Delta t = \pi/8$ then leads to the prediction of $\langle S_2^{(A)} S_3^{(A)}\rangle = \cos(\pi/4)$ [refer Eq. (19)]. This gives violation of the inequality (24), the left side being $\sqrt{2}$.

The above calculations assume large β (and hence orthogonal $|\beta\rangle$ and $|-\beta\rangle$) so that one may justify the assumption that the system A at times t_1 and t_2 is projected into one or other of the states $|\alpha\rangle$ or $|-\alpha\rangle$, once the measurement at B is performed. To evaluate accurately requires evaluation of the joint distributions $P(X_A, X_B)$ for the different times of interaction t_a and t_b. For large α and β, the simplistic result is indeed recovered, for all $\alpha, \beta > 1$. The precise results were calculated in [33], and are given in Fig. 7. The results agree with the moments above, predicting violation of the inequality, for $\alpha > 1$. The plots of $P(X_A, X_B)$ for the various times of evolution are given in Fig. 10.

The violation of the inequality (24) implies falsification of macrorealism. We note that the measurements $S_i^{(A)}$and $S_j^{(B)}$ are macroscopic in the sense that one needs only to distinguish between the two macroscopically separated peaks of the distributions $P(X_A, X_B)$ (Fig. 10). Here, the meaning of "macroscopic" refers to a separation in phase space of quadrature amplitudes X by an arbitrary amount ($\alpha \to \infty$).

C. Interpretation without macroscopic retrocausality

As explained above, macrorealism involves two assumptions: weak macroscopic realism (wMR) and noninvasive measurability. If we assume the validity of wMR, then we would conclude that noninvasive measurability fails: the measurement of the spin $S_i^{(B)}$ of B disturbs the result for the spin $S_j^{(A)}$of A ($j > i$). However, since the measurements are made at B after the state of A at the time t_3 is measured, this conclusion might suggest that the violation of the Leggett-Garg inequality is due to a macroscopic retrocausal effect, where which measurement is made at B alters the past value of λ_i at A.

Here, we show how the dynamics pictured in Fig. 10 provides an interpretation that avoids the conclusion of macroscopic retrocausality. This is done by showing consistency with weak macroscopic realism (wMR) and that the violation of the Leggett-Garg inequality coincides with the failure of deterministic macroscopic realism (dMR).

1. Consistency with weak macroscopic realism: The pointer measurement

In order to demonstrate consistency with weak macroscopic realism (wMR), we first summarize what this assumption implies for the dynamics of the Leggett-Garg test, shown in Figs. 6–11. At each of the times t_j ($j = 1, 2, 3$), the systems

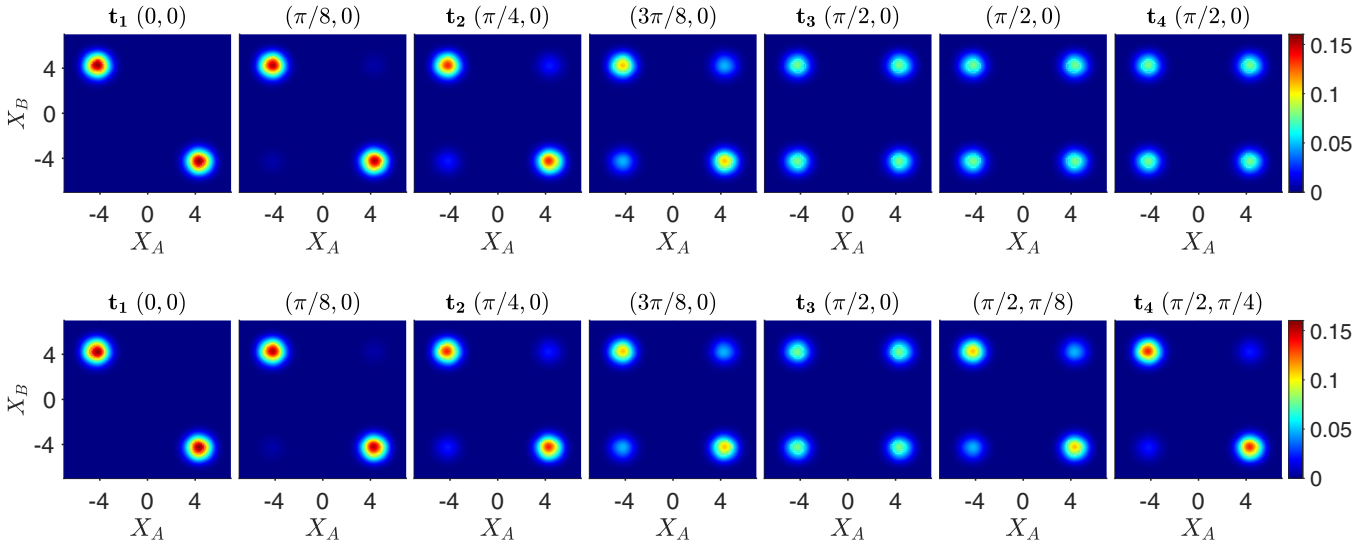

FIG. 10. Contour plots of $P(X_A, X_B)$ showing the dynamics as the state $|\psi_{\text{Bell}}(t_1)\rangle$ evolves through the three measurement sequences of the Leggett-Garg test in the delayed-choice gedanken experiment depicted in Figs. 8 and 9. Here, we go from time $t = t_1$ (far left), through to $t = t_2$ (third picture from left), $t = t_3$ (fifth picture from left), and, finally, $t = t_4$ (far right). The systems evolve locally according to $H_{\text{NL}}^{(A/B)}$ for interaction times t_a and t_b given by (t_a, t_b) in units of Ω^{-1}. Top: The sequence to infer $S_1^{(A)}$ by delayed measurement of $S_1^{(B)}$, enabling measurement of $\langle S_1^{(B)} S_3^{(A)}\rangle = -\langle S_1^{(A)} S_3^{(A)}\rangle$ (final picture), as in Fig. 8 (lower). The sequence to measure $\langle S_1^{(B)} S_2^{(A)}\rangle = -\langle S_1^{(A)} S_2^{(A)}\rangle$ uses $t_a = t_2 = \pi/4$ as in Fig. 8 (top) and ends with the third picture of the sequence. Lower: The sequence to infer $S_2^{(A)}$ by measurement of $S_2^{(B)}$, enabling measurement of $\langle S_2^{(B)} S_3^{(A)}\rangle = -\langle S_2^{(A)} S_3^{(A)}\rangle$ (final picture) as in Fig. 9. Here, $t_1 = 0$, $t_2 = \pi/4$, and $t_3 = \pi/2$. $\alpha = \beta = 3$.

A and B are in an entangled macroscopic superposition of type

$$|\psi_{\text{ent}}\rangle = \mathcal{N}(c_1|\alpha\rangle|-\beta\rangle + c_2|-\alpha\rangle|\beta\rangle + c_3|\alpha\rangle|\beta\rangle + c_4|-\alpha\rangle|-\beta\rangle), \tag{25}$$

where α, $\beta \to \infty$ and c_k are probability amplitudes. This is a superposition of states with definite outcomes for *pointer* measurements $S_j^{(A)}$ and $S_j^{(B)}$, and is an example of a pointer superposition $|\psi_{\text{pointer}}\rangle$. The premise wMR asserts that the system A at the time t_j is in one or the other of two macroscopic states φ_+ and φ_-, for which the result of the spin measurement $S_j^{(A)}$ (given by the sign of the coherent amplitude) is determined to be $+1$ or -1, respectively. Hence, the system A at time t_j may be described by the macroscopic hidden variable $\lambda_j^{(A)}$. The value of $\lambda_j^{(A)}$ is fixed as either $+1$ or -1 at the particular time t_j, prior to the pointer measurement, and is

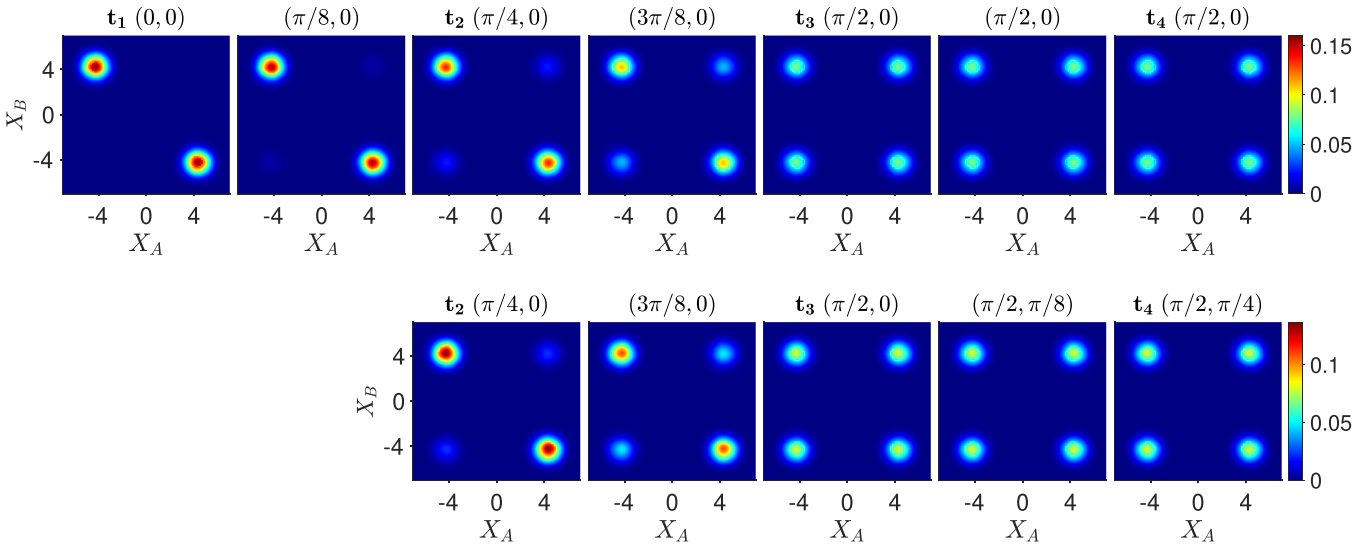

FIG. 11. Contour plots of $P(X_A, X_B)$ showing the dynamics as the *nonentangled* state ρ_{mix} [Eq. (26)] evolves through the same measurement sequences given in Fig. 10. Notation as for Fig. 10. Top: The sequence evolves as in Fig. 8 (lower) with a unitary rotation at site A only. Although starting with ρ_{mix} at time t_1, the sequence is indistinguishable from that given by the top sequence in Fig. 10 for the entangled state $|\psi_{\text{Bell}}(t_1)\rangle$. Lower: We assume the system evolves as for Fig. 9 and the lower sequence of Fig. 10 with two unitary rotations, one at A and one at B, but starting from the nonentangled state ρ_{mix} at the time $t = t_2$. Although indistinguishable at the initial time t_2, the final picture at $t = t_4$ $[(\pi/2, \pi/4)]$ differs macroscopically from that of the entangled state (compare with the lower sequence in Fig. 10).

independent of any future measurement. By the pointer measurement at A, it is meant that the measurement can be made as a final quadrature detection X_A, with *no further unitary rotation* U_A necessary. For the entangled state $|\psi_{\rm ent}\rangle$, similar assumptions apply to system B. Weak macroscopic realism does not (necessarily) imply that prior to the measurement of spin $S^{(A)}$, the system is in the state $|\alpha\rangle$ or $|-\alpha\rangle$, nor in any quantum state. This is because quantum states are microscopically specified, giving predictions for all measurements that might be performed on A, whereas the definition of wMR considers only macroscopic coarse-grained measurements.

The macroscopic predictions for quadrature measurements X_A and X_B performed on the system in the entangled state $|\psi_{\rm ent}\rangle$ [Eq. (25)] are fully consistent with wMR. This is evident on comparing with the predictions for the nonentangled state $\rho_{\rm Mix}$, given by the mixture of the four states $|\alpha\rangle|-\beta\rangle$, $|-\alpha\rangle|-\beta\rangle$, $|\alpha\rangle|\beta\rangle$ and $|-\alpha\rangle|-\beta\rangle$ (the relative probabilities for the mixture being, in order, $|c_1|^2$, $|c_2|^2$, $|c_3|^2$ and $|c_4|^2$). Where $|\psi_{\rm ent}\rangle$ corresponds to the Bell state $|\psi_{\rm Bell}(t_1)\rangle$ of Eq. (8), $\rho_{\rm Mix}$ becomes

$$\rho_{\rm mix} = \tfrac{1}{2}\{|\alpha\rangle|-\beta\rangle\langle-\beta|\langle\alpha| + |-\alpha\rangle|\beta\rangle\langle\beta|\langle-\alpha|\}. \quad (26)$$

The nonentangled state $\rho_{\rm Mix}$ is consistent with wMR, since each subsystem A and B can be viewed as being in one or other of two macroscopically distinct coherent states. We see that there is *no distinguishable difference* between the predictions $P(X_A, X_B)$ for the entangled $[|\psi_{\rm ent}\rangle]$ and nonentangled ($\rho_{\rm Mix}$) states, at the level of the macroscopic outcomes (e.g. compare predictions for $|\psi_{\rm Bell}(t_1)\rangle$ and $\rho_{\rm mix}$ in the first plots of the top sequences in Figs. 10 and 11). A distinction exists, but at order $\hbar e^{-|\alpha|^2}$, invisible on the plots. At each of the times t_j shown in the dynamics associated with the Leggett-Garg test, the system is in a state of the type $|\psi_{\rm ent}\rangle$, which is compatible with wMR as defined for the pointer measurements X_A and X_B.

For the bipartite system, wMR is consistent with a form of macroscopic locality that we call "macroscopic locality of the pointer" (MLP). The meaning of MLP was summarized in [33] and asserts that the value of the macroscopic hidden variable $\lambda_j^{(A)}$, which gives the outcome for the pointer measurement on system A, cannot be changed by any spacelike-separated event, or measurement, at the system B that takes place at time $t \geqslant t_j$, e.g., it cannot be changed by a future event at B. This premise is different to the stronger assumption of macroscopic Bell locality (ML), which is assumed to (also) apply to systems defined prior to the unitary dynamics associated with the measurement settings [32,33].

2. Failure of deterministic macroscopic realism

We next show that the violation of the Leggett-Garg inequality (24) implies a failure of deterministic macroscopic realism (dMR). This premise (different to wMR) asserts a predetermined outcome for the measurement *prior* to the unitary rotation U that determines the measurement setting.

Let us consider the dynamics of Fig. 9, at time t_2. Assuming wMR, the value of $\lambda_2^{(A)}$ is determined at the time t_2 and determines the outcome for the pointer measurement $S_2^{(A)}$. However, one may also consider the outcome of a measurement $S_3^{(A)}$ at the later time, made by applying a rotation $U^{(A)}(\pi/4)$ and then measuring X_A. If we assume dMR, then this latter outcome can also be regarded as determined, and we can assign the hidden variable $\lambda_3^{(A)}$ to the system at the time t_2. Similarly, assuming dMR, one may assign variables $\lambda_2^{(B)}$ and $\lambda_3^{(B)}$ to system B, at time t_2.

Extending this argument, the premise of dMR would imply that the system A at time t_1 can be ascribed simultaneous predetermined values λ_j for all three spin outcomes S_j ($j = 1, 2, 3$), regardless of the future unitary dynamics required to actually perform the measurements, and hence implies the Leggett-Garg inequality (24) to be satisfied. We have shown in Sec. IV B that the Leggett-Garg inequality is predicted to be violated. This implies that dMR is falsifiable by the proposed experiment (Fig. 1).

3. Explanation

The apparent retrocausal effect can be explained as arising from the failure of deterministic macroscopic realism (dMR). In other words, the violations of the Leggett-Garg inequality can be shown to arise as a failure of dMR.

We explain further. First, examining Fig. 10 for the Leggett-Garg violations, we see that the macroscopic dynamics of the sequences for $\langle S_1^{(B)} S_3^{(A)}\rangle$ and $\langle S_1^{(B)} S_2^{(A)}\rangle$ (Fig. 8) involving only one unitary rotation are identical to those of the nonentangled state $\rho_{\rm mix}$ [Eq. (26)]. Where one measures $\langle S_1^{(B)} S_2^{(A)}\rangle$ or $\langle S_1^{(B)} S_3^{(A)}\rangle$, the predictions $P(X_A, X_B)$ for the systems evolving from the entangled $[|\psi_{\rm Bell}(t_1)\rangle]$ and nonentangled ($\rho_{\rm mix}$) states *remain indistinguishable* throughout the dynamics (compare the top sequences of Figs. 10 and 11). This corresponds to there being no rotation (unitary evolution) at site B (Fig. 8). A distinction in fact exists, but at the microscopic level of order $\hbar e^{-|\alpha|^2}$, which is not visible on the plots. These time sequences can therefore be modeled by evolution of $\rho_{\rm mix}$, which gives a dynamics consistent with the macrorealism showing no violation of the Leggett-Garg inequality.

Where one has *two* unitary rotations, one at each site as in Fig. 9, there is no longer consistency with the predictions of $\rho_{\rm mix}$. There is a *macroscopic* difference for the evolution where one measures $\langle S_3^{(A)} S_2^{(B)}\rangle$, which involves *two* unitary rotations after t_2, as depicted in Fig. 9. This is seen by comparing the lower sequences of Figs. 10 and 11. If one starts with a nonentangled state $\rho_{\rm mix}$ at time t_2 [Fig. 11 (lower)], then although the joint probabilities $P(X_A, X_B)$ are indistinguishable at t_2, the joint probabilities differ macroscopically *after* the evolution involving rotations at both sites (compare the last pictures in the lower sequences).

We conclude that the violation of macrorealism and hence the apparent retrocausality arises from the measurement of $\langle S_3^{(A)} S_2^{(B)}\rangle$ (i.e., $\langle S_2^{(A)} S_3^{(A)}\rangle$), as in Fig. 9. In measuring $\langle S_2^{(A)} S_3^{(A)}\rangle$ via $\langle S_2^{(B)} S_3^{(A)}\rangle$, as in the lower sequence of Fig. 10, the system at A is *entangled* with B at time t_2. There is no contradiction with wMR, because the measurement of $\langle S_2^{(B)} S_3^{(A)}\rangle$ involves *two* rotations after the time t_2, one at A and one at B. The premise wMR specifies a predetermined outcome λ_j only for the pointer measurement, and at any given time t_j at a given site, there can only be a preparation with respect to a single pointer measurement, S_J (Fig. 12). The double rotation however allows a failure of deterministic macroscopic realism, as explained in the last section.

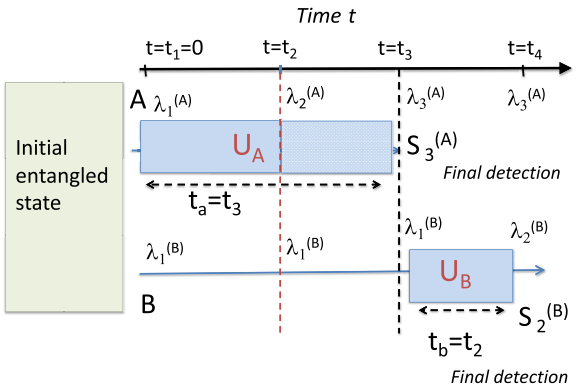

FIG. 12. Consistency with weak macroscopic realism is possible for the time sequence of Fig. 9. The system at time t_1 has valid hidden variables $\lambda_1^{(A)}$ and $\lambda_1^{(B)}$, being indistinguishable from $\rho_{\rm mix}$. At time t_2, system A has valid $\lambda_2^{(A)}$ and $\lambda_1^{(A)}$, the value of $\lambda_1^{(A)}$ being given by the pointer measurement on B at the time t_2. Similarly, system B at time t_2 has valid $\lambda_1^{(B)}$ and $\lambda_2^{(B)}$. At time t_3, the system A has valid $\lambda_3^{(A)}$ and $\lambda_1^{(A)}$, since the value of $\lambda_1^{(A)}$ can be given by the pointer measurement at t_3 on B. At time t_3, system B has valid $\lambda_1^{(B)}$ and $\lambda_3^{(B)}$ (because $\lambda_3^{(B)}$ can be inferred from $\lambda_3^{(A)}$). At time t_4, system A has valid hidden variables $\lambda_3^{(A)}$ and $\lambda_2^{(A)}$.

The assumption of weak macroscopic realism (wMR) implies the following interpretation that assigns hidden variables at each stage in the dynamics, as shown in Fig. 12. Following Fig. 9, the system A at times t_1 and t_2 can be represented by the hidden variables $\lambda_1^{(A)}$ and $\lambda_2^{(A)}$ (meaning that the pointer measurements of $S_1^{(A)}$ and $S_2^{(A)}$ have predetermined outcomes). The argument within the wMR model is that this is justified because the predictions for pointer measurement $S_1^{(A)}$ and $S_2^{(A)}$ are identical with those arising from $\rho_{\rm mix}$ (there has been a rotation at one site, A, only). This is also true of the system B at time t_1: it can be described by a $\lambda_1^{(B)}$, for the reason that the predictions are indistinguishable from those of $\rho_{\rm mix}$. Continuing, wMR implies that at time t_2, A can also be consistently represented by a hidden variable $\lambda_1^{(A)}$ because the value $S_1^{(B)}$ at B is determinable by a pointer measurement, without further rotation. Also, because of the correlation with $S_2^{(A)}$, one would conclude $\lambda_2^{(B)}$ can be assigned to the state B at the time t_2 because the outcome after the unitary evolution $U^{(B)}(\pi/4)$ is predetermined. However, it is *not* the case that at time t_2 the outcome of $S_3^{(A)}$ is predetermined [if $U^{(A)}(\pi/4)$ would be performed] because dMR fails. Hence, at time t_2, it is not true that the hidden variable λ_3 can be assigned to the state at A because the unitary rotation $U^{(A)}(\pi/4)$ has not been performed. Regardless, this does not imply failure of wMR because the dynamics associated with $U^{(A)}(\pi/4)$ is in the future of t_2.

On the other hand, if the unitary rotation $U^{(B)}(\pi/2)$ that precedes the measurement $S_3^{(B)}$ *is* performed *prior* to the time t_2 at B, then the state at A at time t_2 can be assigned $\lambda_3^{(A)}$, but can no longer be assigned $\lambda_1^{A)}$ at that time t_2. This interpretation allows for macroscopic Bell nonlocal effects when there are unitary rotations at both sites, but is also consistent with weak macroscopic realism (wMR) and hence does not indicate macroscopic retrocausality.

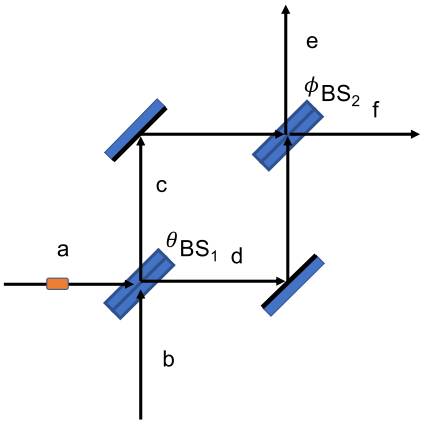

FIG. 13. Schematic of Wheeler-CLP delayed-choice experiment. A single-boson two-mode state $|1\rangle_a|0\rangle_b$ is incident on the BS_1. The first beam splitter introduces a variable reflectivity given by θ with output modes c and d. These two modes are again recombined at a BS_2 to produce final output modes e and f, with a variable transformation angle ϕ.

V. DIMENSION WITNESS TEST

We next follow the approach of Chaves, Lemos, and Pienaar (CLP) [27], by demonstrating violation of the dimension witness inequality [29,30,44–47]. Here, one considers two-dimensional models and, within this framework, confirms the failure of all nonretrocausal models. Our results extend beyond those of CLP because the conclusions of retrocausality apply to the macroscopic qubits $|\alpha\rangle$ and $|-\alpha\rangle$ where α is large, for which the binary outcomes of the relevant measurements are distinguishable beyond $\hbar$. This test makes concrete the apparent retrocausality discussed in Sec. IV C, and elucidates how this can be interpreted as due to the limitation of the assumption of a two-dimensional hidden variable model.

We first consider the Wheeler-CLP delayed-choice experiment performed with tunable beam splitters, which have variable reflectivities. A single boson is incident on the beam splitter, so that the input system is the two-mode state $|1\rangle_a|0\rangle_b$ (Fig. 13). The two modes (c and d) at the outputs of the beam splitter have boson operators

$$\hat{c} = \hat{a}\cos\theta - \hat{b}\sin\theta,$$
$$\hat{d} = \hat{a}\sin\theta + \hat{b}\cos\theta. \tag{27}$$

After the beam splitter, the state of the field in the interferometer is

$$|\psi\rangle_p = a^\dagger|0\rangle_a|0\rangle_b = \cos\theta|1\rangle_c|0\rangle_d + \sin\theta|0\rangle_c|1\rangle_d. \tag{28}$$

This is the preparation state, prepared at time t_1. The fields pass through the interferometer, and are recombined at a second beam splitter to produce final output modes e and f. The beam-splitter transformation

$$\hat{e} = \hat{c}\cos\phi - \hat{d}\sin\phi,$$
$$\hat{f} = \hat{c}\sin\phi + \hat{d}\cos\phi \tag{29}$$

constitutes the measurement, and gives the final state

$$|\psi\rangle_m = \cos(\theta-\phi)|1\rangle_e|0\rangle_f + \sin(\theta-\phi)|0\rangle_e|1\rangle_f. \tag{30}$$

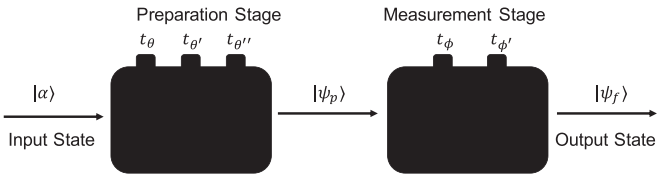

FIG. 14. The setup for a macroscopic Wheeler-CLP delayed-choice experiment where we make use of the cat-state dynamics for a prepare and measure scenario. An initial input of $|\alpha\rangle$ undergoes a nonlinear interaction $H_{\rm NL}$ for a time t_θ at the preparation stage, corresponding to the BS_1. A second interaction $H_{\rm NL}$ is applied for a time t_ϕ at the measurement stage, which corresponds to the BS_2. We make use of a dimension test on the final output to demonstrate failure of two-dimensional nonretrocausal models for the macroscopic system.

The binary outcomes $|1\rangle_c|0\rangle_d$ and $|0\rangle_0|1\rangle_d$ are denoted $b=1$ and -1, respectively. The expectation value for b is $E(\theta,\phi)=\cos^2(\theta-\phi)-\sin^2(\theta-\phi)=\cos[2(\theta-\phi)]$. Certain choices of angles θ and ϕ will violate the dimension witness inequality, as we show below.

We map the above scheme onto a macroscopic system using the cat-state dynamics as shown by Fig. 14. The input state is $|\alpha\rangle$. The nonlinear interaction $H_{\rm NL}$ replaces the beam splitter interaction BS_1. For certain choices of interaction time $t_\theta=m\pi/8$, where m is an integer, the system is prepared in the superposition

$$|\psi\rangle_p=e^{-i\varphi}(\cos\theta|\alpha\rangle+i\,\sin\theta|-\alpha\rangle), \tag{31}$$

where $\theta=t_\theta/2$ and $\varphi=t_\theta/2$ is a phase factor. This is proved in Appendix 3. Here we express time t in units of Ω^{-1}. The measurement stage corresponding to the second beam splitter consists of a second interaction $H_{\rm NL}$ applied for a time t_ϕ, so that

$$\begin{aligned}|\alpha\rangle\rightarrow|\alpha\rangle_t&=e^{-i\varphi_2}(\cos\phi|\alpha\rangle+i\,\sin\phi|-\alpha\rangle),\\ |-\alpha\rangle\rightarrow|-\alpha\rangle_t&=e^{-i\varphi_2}(\cos\phi|-\alpha\rangle+i\,\sin\phi|\alpha\rangle)\end{aligned} \tag{32}$$

for certain choices of ϕ. The final state after the interaction is

$$\begin{aligned}|\psi\rangle_f&=e^{-iH_{\rm NL}t_\phi/\hbar}|\psi\rangle_p\\ &=e^{-i(\varphi+\varphi_2)}[\cos\theta(\cos\phi|\alpha\rangle+i\,\sin\phi|-\alpha\rangle)\\ &\quad+i\,\sin\theta(\cos\phi|-\alpha\rangle+i\,\sin\phi|\alpha\rangle)]\\ &=e^{i\eta}[\cos(\theta+\phi)|\alpha\rangle+i\,\sin(\theta+\phi)|-\alpha\rangle],\end{aligned} \tag{33}$$

where η is a phase factor. Identifying $b=1$ as outcome $|\alpha\rangle$ and $b=-1$ as outcome $|-\alpha\rangle$, we obtain the results

$$E(\theta,\phi)=\cos[2(\theta+\phi)] \tag{34}$$

similar to those obtained for the modified Wheeler-CLP delayed-choice experiment described above. It is emphasized that the expression for $E(\theta,\phi)$ is only true for certain values of θ and ϕ, where (31) and (32) hold.

The setup is an example of a prepare and measure scenario considered by CLP [27]. In their notation, the first measurement setting t_θ is denoted by θ and the second t_ϕ is denoted by ϕ. They derived a dimension witness inequality (DWI) that is satisfied for nonretrocausal models of no more than two dimensions. In our notation, this inequality for the preparation

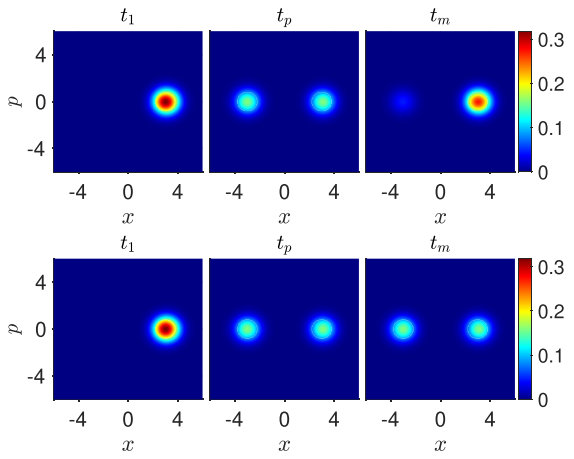

FIG. 15. Contour plots for the Q function $Q(x,p)$ as the system of Fig. 14 evolves from the coherent state $|\alpha\rangle$ at time $t_1=0$. (Top) In this sequence, the first interaction $H_{\rm NL}$ acts for a time $t_2=t_\theta$, preparing the system in the two-state superposition $|\psi\rangle_p$ [Eq. (31)] at the time $t_2=t_p$. This is followed by a second interaction $H_{\rm NL}$ for a time t_ϕ to produce a final state at time $t_3=t_m$. Here, $\theta=\pi/4$ and $\phi=-\pi/8$. (Lower) The lower sequence depicts the system prepared at the time t_p in a mixture of states $|\alpha\rangle$ and $|-\alpha\rangle$. This occurs if the system is measured at that time, in such a way that the system collapses to the mixture. The system then evolves according to $H_{\rm NL}$ for a time t_ϕ to produce the final state at time $t_3=t_m$.

settings θ,θ',θ'' and the measurement settings ϕ,ϕ' is

$$\begin{aligned}I_{\rm DW}=|&E(\theta,\phi)+E(\theta,\phi')+E(\theta',\phi)\\ &-E(\theta',\phi')-E(\theta'',\phi)|\leqslant 3,\end{aligned} \tag{35}$$

where here $E(\theta,\phi)=\cos[2(\theta+\phi)]$. The t_θ and t_ϕ denote the time settings at the respective beam-splitter interactions $H_{\rm NL}$. If we violate DWI, then this indicates failure of all nonretrocausal classical two-dimensional models, therefore implying retrocausality if we are to view the system as observing a two-dimensional classical realist model. For such a classical two-dimensional model, one would conclude that the choice of measurement ϕ affects the earlier state.

It is known that for the solution $E(\theta,\phi)=\cos[2(\theta-\phi)]$ given by Eq. (34), violation of the DW inequality is possible, the maximum value for $I_{\rm DW}$ being $I_{\rm DW}=1+2\sqrt{2}=3.8284$. The angle choices are $\theta=\pi/8$, $\theta'=3\pi/8$, $\theta''=-\pi/4$, $\phi=\pi/4$, $\phi'=0$ [27]. In the macroscopic case where the solution is $E(\theta,\phi)=\cos[2(\theta+\phi)]$, we select $\theta=\pi/8$, $\theta'=3\pi/8$, $\theta''=7\pi/4$, $\phi=7\pi/4$, $\phi'=0$. For these angle choices, the two-state solution (32) holds (refer Appendix 3), as necessary for a macroscopic two-state test. The maximum violation $I_{\rm DW}=1+2\sqrt{2}$ is possible for this choice of angles. We may also select $\theta=\pi/4$, $\theta'=\pi/2$, $\theta''=7\pi/8$, $\phi=13\pi/8$, $\phi'=15\pi/8$.

In Fig. 15, we plot the Q function for the state of the system at the times t_0, t_p, and t_m. The Q function is defined as

$$Q(x,p)=\frac{1}{\pi}\langle\alpha_0|\rho|\alpha_0\rangle, \tag{36}$$

where $|\alpha_0\rangle$ is a coherent state, and $\alpha_0=x+ip$. The two-state dynamics is evident, as the system evolves under the action of $H_{\rm NL}$. The $H_{\rm NL}$ provides the rotation into the superposition

state, in analogy to the beam-splitter interaction. Also plotted in Fig. 15 is the Q function where the system at the time t_p is prepared in a mixture of $|\alpha\rangle$ and $|-\alpha\rangle$. This applies where the system in the superposition at t_p is measured, so that an experimentalist may determine which of the two states the system was in at the time t_p (according to the macro-realist model). In fact, the Q function for the superposition (top graph) differs from that of the mixture (lower graph) by terms of order $e^{-|\alpha|^2}$. For $\alpha > 1$, this difference is not visually noticeable on the scale of the plots. It is noted, however, that after the subsequent rotation $H_{\rm NL}^{\phi}$ ($\phi \neq 0$), the Q functions provided from the superposition (top graph at time t_m) and the mixture (lower graph at t_m) are *macroscopically* distinguishable.

The Q function $Q(x, p)$ corresponds to antinormally ordered moments, and hence does not directly correspond to the measured probabilities for x and p at the microscopic level of $\hbar$. However, at the macroscopic level where one distinguishes between the two states $|\alpha\rangle$ and $|-\alpha\rangle$, the Q function accurately depicts the relative probabilities, i.e., the weighting of the two peaks as pictured in the plots corresponds to the relative probabilities for the binary outcomes $b = 1$ and -1. The extra terms of order $e^{-|\alpha|^2}$ are negligible.

The violation of the dimension witness inequality indicates failure of two-dimensional nonretrocausal wMR models. This is not inconsistent with the nonretrocausal interpretation given by Sec. IV C because the phase-space dynamics relies on a continuum of values for X and P. At time $t_2 = t_p$, there is no distinction between the *macroscopic* two-state depictions $Q(x, p)$ (compare also the pictures at t_2 for the lower sequences of Figs. 10 and 11). Yet, there are differences of order $\hbar e^{-|\alpha|^2}$. It is due to these microscopic differences between the superposition (entangled) and mixed (nonentangled) states, evident in the full phase-space distribution at t_2, that there is a different dynamics, leading to a macroscopic difference in $E(\theta, \phi)$ at the later time $t_3 = t_m$.

VI. WEAK MACROSCOPIC REALISM AND EPR PARADOXES AT A MICROSCOPIC LEVEL

In the previous sections, we show how to realize macroscopic paradoxes involving Leggett-Garg and dimension witness inequalities. While there is a contradiction between deterministic macroscopic realism (dMR) and quantum mechanics for these paradoxes, inconsistency with weak macroscopic realism (wMR) is not demonstrated at this macroscopic level. However, inconsistencies arise at the microscopic level.

In this section, we show that at a *microscopic* level where measurements resolve at the level of $\hbar$, the premises of wMR and local causality give EPR-type paradoxes [37]. This implies that there is inconsistency between each of these premises and the *completeness* of quantum mechanics. EPR paradoxes involving local causality have been illustrated previously for macroscopic superpositions of type [69,70]

$$|\psi\rangle = \frac{1}{\sqrt{2}}(|\alpha\rangle|\uparrow\rangle + |-\alpha\rangle|\downarrow\rangle), \tag{37}$$

often taken as an example of a "Schrödinger cat" state [71–73]. The approach here is similar since for large β, the coherent states $|\beta\rangle$ and $|-\beta\rangle$ are orthogonal qubits.

A. EPR paradox using local causality

We consider the bipartite system prepared in the Bell state

$$|\psi_{\rm Bell}\rangle = \frac{1}{\sqrt{2}}(|\alpha\rangle|-\beta\rangle - |-\beta\rangle|\alpha\rangle) \tag{38}$$

at time t_2, as for (14). The original EPR argument shows incompatibility between the premise of local realism and the completeness of quantum mechanics [37]. The EPR argument was generalized to allow for imperfect correlation between the two sites in [74], including for spin systems in [75,76]. Here, we apply this generalization to illustrate the paradox for the entangled Bell cat state.

The EPR argument considers the prediction for X_A, given a measurement at B. For large β, a measurement of $S_2^{(B)}$ at B will "collapse" system A to the quantum state $|\alpha\rangle$ or $|-\alpha\rangle$, implying a variance $(\Delta X_A)^2 = \frac{1}{2}$ for A, conditioned on the result for $S_2^{(B)}$. We write this conditional variance as $\Delta_{\rm inf}^2 X_A \equiv (\Delta_{\rm inf} X_A)^2 = \frac{1}{2}$, the variance for the inference of X_A given the measurement at B.

The EPR argument then considers the prediction for P_A of system A at time t_2, as can be inferred from a measurement made at B. Here, we propose that the measurement made at B be given by $U_B(t_2)^{-1}$ followed by a measurement of $S_2^{(B)}$ (the sign of X_B). The state after the transformation $U_B(t_2)^{-1}$ is (15), and the measurement of $S_2^{(B)}$ allows an inference of the value of P_A, of system A at time t_2. The measurement of $S_2^{(B)}$ at B "collapses" system A to either $U_{\pi/8}^{(A)}|\alpha\rangle$ or $U_{\pi/8}^{(A)}|-\alpha\rangle$. Following the method of [74], the inferred statistics is thus given by $U_{\pi/8}^{(A)}|\alpha\rangle$ or $U_{\pi/8}^{(A)}|-\alpha\rangle$, which are superpositions (16) of $|\alpha\rangle$ or $|-\alpha\rangle$, and for which the conditional distributions are $P_+(P_A)$ and $P_-(P_A)$ of Eq. (17), respectively. These distributions show fringes, and have the variance $\Delta_{\rm inf}^2 P_A$ for P. This variance of the inferred value for P_A is [70]

$$\Delta_{\rm inf}^2 P_A = \tfrac{1}{2} - |\alpha|^2 e^{-4|\alpha|^2}. \tag{39}$$

The level of combined inference is

$$\varepsilon = \Delta_{\rm inf} X_A \Delta_{\rm inf} P_A < \tfrac{1}{2}, \tag{40}$$

which is below the value for the uncertainty principle $\Delta X_A \Delta P_A \geqslant \frac{1}{2}$, thus implying an EPR paradox [74].

It is also known that the observation of (40) demonstrates an EPR steering [77–80]. If Bell's premise of *local causality* is assumed valid, the condition (40) is paradoxical because it implies that the system A cannot be specified as being in any mixture of localized *quantum* states φ_+ or φ_- (since such states would need to violate the uncertainty principle) [77–80]. This negates the hypothesis that the system of (38) can be regarded as being in either $|\alpha\rangle$ or $|-\alpha\rangle$ (or indeed in any φ_+ or φ_- if these are to be quantum states) in a way that is consistent with local causality. The original EPR paradox assumes local realism, a more specific form of local causality useful when one has perfectly correlated results for both conjugate measurements.

In the above prediction for the EPR inequality, it is assumed that an idealized measurement at B "collapses" system A into one or other of the coherent states. In a more rigorous analysis, we evaluate the conditional statistics for system A using the specific proposal for the measurement at B, where the sign of X_B is measured, as in the calculations of Sec. IV.

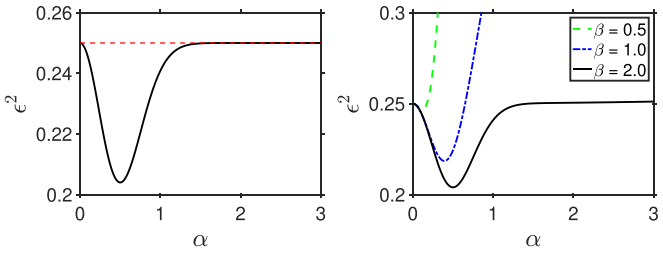

FIG. 16. Plots showing the violation of the macroscopic EPR inequality (40). We first plot (left) $\mathcal{E}^2$ given by Eq. (39). The same result is given for $\mathcal{E}^2_M$ which defines the macroscopic paradox, Eq. (43). The second plot (right) shows the full calculation for $\mathcal{E}^2$ given by Eqs. (41) and (42) based on the proposed method to measure β using X_B, which becomes optimal when β is sufficiently large. Here, we show $\mathcal{E}^2$ versus α for $\beta = 0.5$, 1, and 2.

This gives for the state (14) an inference variance in X_A of

$$\Delta^2_{\rm inf} X_A = \frac{1}{2} + \frac{2|\alpha|^2}{(1 - e^{-2|\alpha|^2 - 2|\beta|^2})} - \frac{2|\alpha|^2 {\rm erf}(\sqrt{2}|\beta|)^2}{(1 - e^{-2|\alpha|^2 - 2|\beta|^2})^2}. \tag{41}$$

The full details are given in Appendices 1 and 2. Similarly, the inferred variance for P is calculated assuming the state (15). We find

$$\Delta^2_{\rm inf} P_A = \frac{1}{2} + \frac{2|\alpha|^2}{(e^{2|\alpha|^2 + 2|\beta|^2} - 1)} - \frac{|\alpha|^2 {\rm erf}(\sqrt{2}|\beta|)^2}{\{e^{2|\alpha|^2} - e^{-2|\beta|^2}\}^2}. \tag{42}$$

In the limit of large β, where the measurement becomes ideal, we see that $\Delta^2 X_A \to \frac{1}{2}$ and $\Delta^2 P_A$ reduces to (39), consistent with the arguments above. Figures 16 and 17 plot ε^2 for varying β. The results become indistinguishable from the ideal case for larger β.

B. EPR paradox based on weak macroscopic realism

The original EPR paradox argues the incompleteness of quantum mechanics based on the assumption of local realism, or local causality, as above. One may also argue an EPR paradox based on the validity of weak macroscopic realism [33]. We summarize this result, for the purpose of comparison.

The cat state for system A is the superposition $c_+|\alpha\rangle + ic_-|-\alpha\rangle$ (for α large), where c_+ and c_- are real probability amplitudes. Weak macroscopic realism (wMR) postulates that the system A in such a state is actually in one or other state φ_+ and φ_- for which the value of the macroscopic spin $S_2^{(A)}$ is

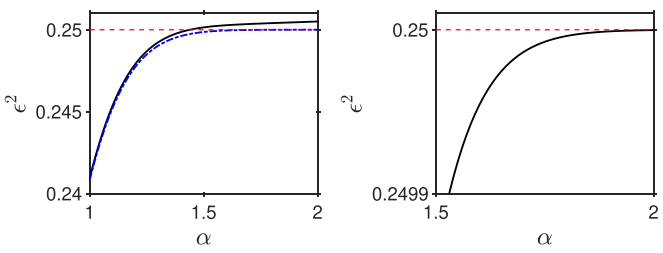

FIG. 17. Plots showing the violation of the macroscopic EPR inequality (40). The notation is as for Fig. 16. Here, we give a closeup of results for the full calculation showing the cutoff values of β needed for $\mathcal{E}^2 < \frac{1}{4}$, for larger α.

determined. While there is a macroscopic separation between the two outcomes, there remains a constraint on the range of X_A that is allowed for the states φ_+ and φ_-. The spin $S_2^{(A)}$ is measured from the quadrature amplitude X_A (as the sign of X_A). The distribution $P(X_A)$ for X_A gives two distinct Gaussian hills, each with variance $(\Delta X_A)^2 = \frac{1}{2}$ [34]. Following [33], one may specify the variance of X_A for the states φ_+ and φ_-. We denote the specified variances as $(\Delta X_A)^2_+$ and $(\Delta X_A)^2_-$, respectively. With the assumption that φ_+ and φ_- are to be *quantum* states, the uncertainty relation $(\Delta X_A)(\Delta P_A) \geqslant \frac{1}{2}$ applies to each state. Then, as explained in [38], for systems in a classical mixture of states φ_+ and φ_- (with respective probabilities P_+ and P_-), it is readily proved that $(\Delta X_A)_{\rm ave}(\Delta P_A) \geqslant \frac{1}{2}$, where $(\Delta X_A)^2_{\rm ave} = P_+(\Delta X_A)^2_+ + P_-(\Delta X_A)^2_-$. The violation of

$$\varepsilon_M \equiv (\Delta X_A)_{\rm ave}(\Delta P_A) \geqslant 1/2 \tag{43}$$

will therefore imply incompatibility of wMR with the completeness of quantum mechanics, since in this case the states φ_+ and φ_- cannot be represented as quantum states. Since here $(\Delta X_A)_{\rm ave} \to \frac{1}{2}$ [or more precisely $(\Delta X_A)_{\rm ave} \not> \frac{1}{2}$], we find the inequality (43) is violated for $(\Delta P_A)^2 < \frac{1}{2}$. This is the case for the Leggett-Garg gedanken experiment, where the distribution $P(P_A)$ at times t_2 and t_3 is given by Eq. (17). The variance is [70]

$$(\Delta P_A)^2 = \tfrac{1}{2} - \alpha^2 e^{-4\alpha^2}. \tag{44}$$

The violation is plotted in Figs. 16 and 17.

C. Discussion

In conclusion, if one assumes weak macroscopic realism (wMR) for the state in a superposition of $|\alpha\rangle$ and $|-\alpha\rangle$, then the fringe distributions shown in Fig. 5 do *not* indicate that the system cannot be regarded as having a definite value for the macroscopic spin (as sometimes interpreted). Rather, the fringes signify that those states φ_+ or φ_- which would have definite macroscopic spin values (if defined consistently with wMR) cannot be given as *quantum* states. There is an incompleteness of quantum mechanics, if wMR is to be valid.

The original EPR paradox concluded inconsistency between local realism and the completeness of quantum mechanics [37]. Bell later showed that local realism itself can be falsified [36]. Similarly, the EPR paradox of Sec. VI A shows inconsistency between local causality (at the level of $\hbar$) and the completeness of quantum mechanics. However, the assumption of local causality has also been falsified, based on Bell theorems [40,41], thereby apparently resolving the paradox. By contrast, the EPR-type paradox explained in Sec. VI B is not readily resolved in the same manner. This paradox shows inconsistency between wMR and the completeness of quantum mechanics [33]. However, there is to date no obvious way to falsify wMR. The paradox involving weak macroscopic realism is hence different and stronger.

While this paper studies the EPR paradox associated with a macroscopic superposition state constructed from coherent states, similar EPR paradoxes have been formulated for other types of macroscopic superposition states, e.g., for NOON states [81,82] and Greenberger-Horne-Zeilinger

(GHZ) states [70,83]. However, these paradoxes give inconsistencies for local causality, or local realism. Less is known about paradoxes that illustrate the inconsistency between weak macroscopic realism and the incompleteness of quantum mechanics, although related examples were given for number-state superpositions in [38]. We expect such paradoxes may also be possible for NOON and GHZ states, and for the higher-dimensional extensions of the GHZ states [84–86].

The method of "irrealism" also gives a way to investigate the incompleteness of quantum mechanics along the lines proposed by EPR [87]. In fact, recent work applies this concept to analyse the double slit experiment [88].

VII. CONCLUSION

In this paper, we have illustrated how one may perform delayed-choice experiments using superpositions of two coherent states. We map the original proposals involving spin qubits ($|\uparrow\rangle$ and $|\downarrow\rangle$) onto macroscopic tests, where the qubits are coherent states $|\alpha\rangle$ and $|-\alpha\rangle$ ($\alpha \to \infty$). In the mapping, the choice to measure a particular spin component corresponds to a choice of interaction time for a unitary transformation realized by a nonlinear Hamiltonian. We also outline Einstein-Podolsky-Rosen–type tests that suggest the incompleteness of quantum mechanics based on the premises of macroscopic realism.

A summary of the models of macroscopic realism that are negated by the predictions of the experiments proposed in this paper is given in Sec. II. In order to counter interpretations that would suggest macroscopic retrocausality, we have demonstrated consistency of the predictions with the concept of weak macroscopic realism (wMR). We find, however, a direct negation of deterministic macroscopic realism (dMR). We also find it possible to negate models consistent with weak macroscopic realism (wMR) that are limited to two dimensions, or else that postulate the underlying macroscopically distinct states in the definition of wMR to be quantum states.

The conclusions possible for each of the experiments proposed in this paper are consistent but complementary. In Sec. III, we presented a version of the delayed-choice quantum eraser experiment, using entangled cat states. The loss of which-way information shows as interference fringes in distributions for the quadrature phase amplitude P. We argued the signature is at the microscopic level of $\hbar$ (since the fringes must be finely resolved) and hence that there is no evidence of macroscopic retrocausality.

Motivated further, in Sec. IV we examined a delayed-choice version of a bipartite macroscopic Leggett-Garg test for the entangled cat states. Here, the measurements are macroscopically coarse grained and the test explicitly demonstrates failure of macrorealism. Macrorealism combines wMR with the assumption of noninvasive measurability at a macroscopic level. The delayed-choice nature of the measurement is then suggestive of an apparent macroscopic retrocausality. We countered this interpretation by showing how the violation of the Leggett-Garg inequality can be explained using the concept of deterministic macroscopic realism (dMR). The premise of dMR is stricter than that of wMR. We showed that the violation falsifies dMR but can be viewed consistently with wMR, thus avoiding the interpretation of macroscopic retrocausality. The nonretrocausal interpretation is supported by the observation that the failure of macrorealism (and dMR) occurs for this bipartite system only where there is unitary dynamics after preparation (in the form of basis rotations that determine the measurement settings) at *both* sites.

In Sec. V, the apparent macroscopic retrocausality of the Leggett-Garg setup is demonstrated in a concrete way, by showing violation of the dimension witness inequality, as in the work of Chaves, Lemos, and Pienaar [27]. This implies failure of all two-dimensional nonretrocausal wMR models. It is explained, however, that one may avoid the conclusion of macroscopic retrocausality, if one allows for higher dimensions within the wMR model. This is consistent with the observation that the nonclassical dynamics of the cat states involves a continuum of variables.

We further showed in Sec. VI that, although the macroscopic experiments are consistent with weak macroscopic realism (wMR), EPR paradoxes exist for measurements giving a microscopic resolution. The paradoxes demonstrate the incompleteness of quantum mechanics, based on the assumptions of either local causality (as applied to cat states), or else wMR. The paradox based on wMR is a strong paradox, because it has not been shown that wMR is falsifiable.

It is interesting to consider the prospect of an experiment. The two-mode entangled cat states have been generated [48,89,90]. The significant challenge is to realize the unitary rotation, which is given by the Hamiltonian $H_{\rm NL} = \Omega\hat{n}^4$ with a quartic dependence on the field boson number. The quantum eraser can be carried out more straightforwardly, using the interaction $H_{\rm NL} = \Omega\hat{n}^2$, which has been experimentally achieved as a Kerr nonlinearity [49,50]. Realizations may also be possible using NOON states and nonlinear beam-splitter interactions [32], or Greenberger-Horne-Zeilinger states and CNOT gates [91].

Finally, we point out that, similar to other delayed-choice tests, the Leggett-Garg test proposed in this paper could be performed with microscopic or photonic Bell states, where the unitary rotations are carried out in the standard way using polarizing beam splitters. The motivation of the proposal using cat states is to more strongly justify interpretations that avoid conclusions of macroscopic retrocausality. Nonetheless, an analogous interpretation of the experiments involving the standard *microscopic* qubit states $|\uparrow\rangle$ and $|\downarrow\rangle$ is also possible. In this interpretation, the system is prepared after the unitary interaction that determines the measurement setting in a superposition of pointer states which have a definite spin value. Within that interpretation, a realism is assigned to this system: the system is in a state with a definite value for the final pointer measurement. The apparent retrocausality can then be explained as a failure of deterministic (local) realism, where the values of spin are assumed to be determined prior to the unitary interaction.

ACKNOWLEDGMENTS

This research has been supported by the Australian Research Council Discovery Project Grants schemes under Grant No. DP180102470. The authors also wish to thank NTT Research for their financial and technical support.

APPENDIX

1. Quantum eraser and EPR calculation

Here, we give details for the superposition $U_{\pi/8}|\pm\alpha\rangle = e^{-i\pi/8}\{\cos\pi/8|\pm\alpha\rangle + i\,\sin\pi/8|\mp\alpha\rangle\}$ examined in Sec. III. The calculations for the superposition $U_{\pi/4}|\pm\alpha\rangle$ are similar.

It is straightforward to evaluate $P(P_A)_+ = |\langle P_A|U_{\pi/8}|\alpha\rangle|^2$ and $P(P_A)_- = |\langle P_A|U_{\pi/8}|-\alpha\rangle|^2$ for the simple case. For the accurate calculation based on the actual measurements that would be used, one considers $|\psi(t_4)\rangle$ and evaluates $P(P_A, X_B) = |\langle X_B|\langle P_A|\psi(t_4)\rangle|^2$:

$$P(P_A, X_B) = 2\frac{\exp(-P_A^2 - X_B^2 - 2|\beta|^2)}{\pi(1 - e^{-2|\alpha|^2-2|\beta|^2})}\left\{\sin^2(\sqrt{2}P_A|\alpha|) + \sinh^2(\sqrt{2}X_B|\beta|) - \frac{\sqrt{2}}{4}\sin(2\sqrt{2}P_A|\alpha|)\sinh(2\sqrt{2}X_B|\beta|)\right\}. \tag{A1}$$

This gives the result (18) using $P(P_A)_\pm = P(P_A|X_B \gtrless 0)$ and

$$P(X_B) = \int P(P_A, X_B)dP_A = \frac{\exp(-X_B^2 - 2|\beta|^2)}{\sqrt{\pi}(1 - e^{-2|\alpha|^2-2|\beta|^2})}\left(1 - e^{-2|\alpha|^2} + 2\,\sinh^2(\sqrt{2}X_B|\beta|)\right). \tag{A2}$$

To evaluate the EPR correlations, we calculate the variance of $P(P_A)_\pm$. We find for the simple analysis

$$\begin{aligned}
\int P_A P(P_A)_\pm dP_A &= \frac{1}{\pi^{1/2}}\left\{\int P_A e^{-P_A^2}dP_A \mp \frac{1}{\sqrt{2}}\int P_A e^{-P_A^2}\sin(2\sqrt{2}P_A|\alpha|)dP_A\right\} \\
&= \frac{1}{\pi^{1/2}}\left\{0 \mp \frac{1}{\sqrt{2}}\sqrt{2}\sqrt{\pi}|\alpha|e^{-2|\alpha|^2}\right\} = \mp|\alpha|e^{-2|\alpha|^2}, \\
\int P_A^2 P(P_A)_\pm dP_A &= \frac{1}{\pi^{1/2}}\left\{\int P_A^2 e^{-P_A^2}dP_A \mp \frac{1}{\sqrt{2}}\int P_A^2 e^{-P_A^2}\sin(2\sqrt{2}P_A|\alpha|)dP_A\right\} \\
&= \frac{1}{\pi^{1/2}}\left\{\frac{\sqrt{\pi}}{2} \mp 0\right\} = \frac{1}{2}
\end{aligned} \tag{A3}$$

which gives the result (39). For the complete measurement, we use the full result (18) for $P(P_A)_\pm$. Integration gives

$$\int P_A P(P_A)_\pm dP_A = \mp\frac{|\alpha|\mathrm{erf}(\sqrt{2}|\beta|)}{\{e^{2|\alpha|^2} - e^{-2|\beta|^2}\}}, \quad \int P_A^2 P(P_A)_\pm dP_A = \frac{1}{2} + \frac{2|\alpha|^2}{(e^{2|\alpha|^2+2|\beta|^2} - 1)} \tag{A4}$$

leading to (42).

2. Calculation of EPR correlations

We first evaluate $\Delta_{inf}^2 X_A$ for the state (14). The inferred variance is defined as

$$\Delta_{\mathrm{inf}}^2 X_A = P(X_B > 0)\Delta_+^2 X_A + P(X_B \leqslant 0)\Delta_-^2 X_A, \tag{A5}$$

where clearly $P(X_B > 0) = \frac{1}{2}$. The conditional distributions are defined

$$P_+(X_A) = P(X_A|X_B > 0) = \frac{\int_0^\infty P(X_A,X_B)dX_B}{\int_0^\infty P(X_B)dX_B} \tag{A6}$$

and similarly $P_-(X_A) = P(X_A|X_B \leqslant 0)$, which, after evaluation of $P(X_A, X_B)$ for the entangled cat state, gives

$$P(X_A)_\pm = \frac{2\mathcal{N}^2 e^{-X_A^2-2|\alpha|^2}}{\sqrt{\pi}}\{\cosh(2\sqrt{2}|\alpha|X_A) \mp \mathrm{erf}(\sqrt{2}|\beta|)\sinh(2\sqrt{2}|\alpha|X_A) - e^{-2|\beta|^2}\}. \tag{A7}$$

The variance of these distributions is $\Delta^2_{\pm}\hat{X}_A = \langle \hat{X}_A^2\rangle - \langle \hat{X}_A\rangle^2$ where

$$\langle \hat{X}_A\rangle_{\pm} = \int P_{\pm}(X_A)X_A dX_A = \frac{\mp\sqrt{2}|\alpha|\mathrm{erf}(\sqrt{2}|\beta|)}{\left(1-e^{-2|\alpha|^2-2|\beta|^2}\right)},$$
$$\left\langle \hat{X}_A^2\right\rangle_{\pm} = \int P_{\pm}(X_A)X_A^2 dX_A = \frac{1}{2} + \frac{2|\alpha|^2}{\left(1-e^{-2|\alpha|^2-2|\beta|^2}\right)}. \tag{A8}$$

This leads to the result

$$\Delta^2_{\mathrm{inf}}X_A = \frac{1}{2} + 4\mathcal{N}^2|\alpha|^2 - 8\mathcal{N}^4|\alpha|^2\mathrm{erf}(\sqrt{2}|\beta|)^2 = \frac{1}{2} + \frac{2|\alpha|^2}{(1-e^{-2|\alpha|^2-2|\beta|^2})} - \frac{2|\alpha|^2\mathrm{erf}(\sqrt{2}|\beta|)^2}{(1-e^{-2|\alpha|^2-2|\beta|^2})^2}. \tag{A9}$$

Similarly, we evaluate $\Delta^2_{inf}P_A$ for the state (15). Here,

$$\Delta^2_{\mathrm{inf}}P_A = P(X_B>0)\Delta^2_{+}P_A + P(X_B\leqslant 0)\Delta^2_{-}P_A.$$

We first evaluate evaluate the conditional distributions of

$$P_{+}(P_A) = P(P_A|X_B>0) = \frac{\int_0^{\infty}P(P_A,X_B)dX_B}{\int_0^{\infty}P(X_B)dX_B} \tag{A10}$$

and, similarly, $P_{+}(P_A) = P(P_A|X_B\leqslant 0) = \frac{\int_0^{\infty}P(P_A,X_B)dX_B}{\int_{-\infty}^{0}P(X_B)dX_B}$ using

$$P(P_A,X_B) = |\langle X_B|\langle P_A|\psi(t_4)\rangle|^2 = \frac{e^{-P_A^2}}{\sqrt{\pi}\{1-e^{-2|\alpha|^2-2|\beta|^2}\}}\left\{1-e^{-2|\beta|^2}\cos(2\sqrt{2}P_A|\alpha|) - \frac{\sqrt{2}}{2}\mathrm{erf}(\sqrt{2}|\beta|)\sin(2\sqrt{2}P_A|\alpha|)\right\}. \tag{A11}$$

This gives

$$P_{\pm}(P_A) = \frac{2\mathcal{N}^2e^{-P_A^2}}{\sqrt{\pi}}\left\{1-e^{-2|\beta|^2}\cos(2\sqrt{2}P_A|\alpha|) \mp \frac{\sqrt{2}}{2}\mathrm{erf}(\sqrt{2}|\beta|)\sin(2\sqrt{2}P_A|\alpha|)\right\}. \tag{A12}$$

Hence,

$$\langle \hat{P}_A\rangle_{\pm} = \int P_{\pm}(P_A)P_A dP_A = \mp\frac{|\alpha|e^{-2|\alpha|^2}\mathrm{erf}(\sqrt{2}|\beta|)}{\{1-e^{-2|\alpha|^2-2|\beta|^2}\}}, \quad \left\langle \hat{P}_A^2\right\rangle_{\pm} = \int P_{\pm}(P_A)P_A^2 dP_A = \frac{1}{2} + \frac{2|\alpha|^2}{\{e^{2|\alpha|+2|\beta|^2}-1\}} \tag{A13}$$

which leads to

$$\Delta^2_{\mathrm{inf}}P_A = \frac{1}{2} + 4\mathcal{N}^2|\alpha|^2e^{-2|\alpha|-2|\beta|^2} - 4\mathcal{N}^4|\alpha|^2e^{-4|\alpha|^2}\mathrm{erf}(\sqrt{2}|\beta|)^2 = \frac{1}{2} + \frac{2|\alpha|^2e^{-2|\alpha|-2|\beta|^2}}{\{1-e^{-2|\alpha|^2-2|\beta|^2}\}} - \frac{|\alpha|^2e^{-4|\alpha|^2}\mathrm{erf}(\sqrt{2}|\beta|)^2}{\{1-e^{-2|\alpha|^2-2|\beta|^2}\}^2}. \tag{A14}$$

3. Cat-state dynamics for the dimension witness test

In this section we consider the two-state solution for the dynamically evolved macroscopic cat states under a nonlinear interaction. Considering α to be real, for an initial coherent state $|\alpha\rangle$ undergoing an evolution with a nonlinear interaction H_{NL}, the state created after an interaction time t_θ can be written as

$$|\alpha,t_\theta\rangle = \exp\left[-\frac{|\alpha|^2}{2}\right]\sum_{n=0}^{\infty}\alpha^n\frac{\exp(-i\Omega t_\theta n^k)}{\sqrt{n!}}|n\rangle. \tag{A15}$$

We restrict to $k=4$. Let us constrain to $t_\theta = m\pi/8$ where m is an integer and choose the units of time such that $\Omega=1$. To obtain the two-state solution in terms of $|\alpha\rangle$ and $|-\alpha\rangle$, we require solutions of type

$$\exp\left[-\frac{|\alpha|^2}{2}\right]\sum_n\alpha^n\frac{\exp(-im\frac{\pi}{8}n^4)}{\sqrt{n!}}|n\rangle = \exp\left[-\frac{|\alpha|^2}{2}\right]\sum_n A\frac{\alpha^n}{\sqrt{n!}}|n\rangle + \exp\left[-\frac{|\alpha|^2}{2}\right]\sum_n B\frac{(-1)^n\alpha^n}{\sqrt{n!}}|n\rangle, \tag{A16}$$

where A and B are constants. Now since the summation indices are the same, this requires $\exp(-im\frac{\pi}{8}n^4) = A+(-1)^nB$. By assigning $n=0,1$ we find $A+B=1$ and $e^{-im\frac{\pi}{8}} = A-B$, giving the solutions as

$$A = e^{-im\frac{\pi}{16}}\cos\left(m\frac{\pi}{16}\right), \quad B = ie^{-im\frac{\pi}{16}}\sin\left(m\frac{\pi}{16}\right). \tag{A17}$$

Hence, we propose that for all integers n such that $n=0,1,2,\ldots$

$$\exp\left(-im\frac{\pi}{8}n^4\right) = e^{-im\frac{\pi}{16}}\left[\cos\left(m\frac{\pi}{16}\right) + (-1)^n i\,\sin\left(m\frac{\pi}{16}\right)\right]. \tag{A18}$$

We now prove this to be true. For even n, we see that the right side of Eq. (A18) satisfies RHS $= 1$. We can write $n = 2J$ where $J = 1, 2, \ldots$ in which case $n^4 = (2J)^4 = 16J^4$. Then we see that the left side (LHS) of Eq. (A18) satisfies LHS $= 1$, since m is an integer. Next we consider odd n. We see that RHS $= e^{-im\frac{\pi}{8}}$. We can write $n = 2J + 1$, where J is an integer, $J \geqslant 1$. We now show that $n^4 = (2J + 1)^4 = 16M + 1$, where M is integer. This is proved by considering $(2J + 1)^4 = 16J^4 + 32J^3 + 24J^2 + 8J + 1$ from which we see that the condition holds if J is even. Then also $(2J + 1)^4 - 1 = 16\{J^4 + 2J^3 + \frac{J}{2}(3J + 1)\}$. This gives the result since $3J + 1$ is even if J is odd and the term $\{J^4 + 2J^3 + \frac{J}{2}(3J + 1)\}$ becomes an integer for all values of J. Hence, LHS $= \exp(-im\frac{\pi}{8})$. Hence, we can write a two-state solution for time multiples of $\pi/8$, as

$$|\alpha, t_\theta\rangle = e^{-it_\theta/2}[\cos(t_\theta/2)|\alpha\rangle + i\,\sin(t_\theta/2)|-\alpha\rangle], \tag{A19}$$

where $t_\theta = m\frac{\pi}{8}$.

[1] J. A. Wheeler, The "past" and the "delayed-choice" double-slit experiment, in *Mathematical Foundations of Quantum Theory*, edited by A. R. Marlow (Academic, New York, 1978), pp. 9–48.

[2] J. A. Wheeler, in *Quantum Theory and Measurement*, edited by J. A. Wheeler and W. H. Zurek (Princeton University Press, Princeton, NJ, 1984), pp. 192–213.

[3] X.-S. Ma, J. Kofler, and A. Zeilinger, Delayed-choice gedanken experiments and their realizations, Rev. Mod. Phys. **88**, 015005 (2016).

[4] M. O. Scully and K. Drühl, Quantum eraser: A proposed photon correlation experiment concerning observation and 'delayed choice' in quantum mechanics, Phys. Rev. A **25**, 2208 (1982).

[5] M. O. Scully, B.-G. Englert, and H. Walther, Quantum optical tests of complementarity, Nature (London) **351**, 111 (1991).

[6] T. J. Herzog, P. G. Kwiat, H. Weinfurter, and A. Zeilinger, Complementarity and the Quantum Eraser, Phys. Rev. Lett. **75**, 3034 (1995).

[7] Y.-H. Kim, R. Yu, S. P. Kulik, Y. Shih, and M. O. Scully, Delayed Choice Quantum Eraser, Phys. Rev. Lett. **84**, 1 (2000).

[8] S. P. Walborn, M. O. Terra Cunha, S. Pádua, and C. H. Monken, Double-slit quantum eraser, Phys. Rev. A **65**, 033818 (2002).

[9] V. Jacques, E. Wu, F. Grosshans, F. Treussart, P. Grangier, A. Aspect, and J.-F. Roch, Experimental realization of wheelers delayed-choice gedanken experiment, Science **315**, 5814 (2007).

[10] A. G. Manning, R. I. Khakimov, R. G. Dall, and A. G. Truscott, Wheeler's delayed-choice gedanken experiment with a single atom, Nat. Phys. **11**, 539 (2015).

[11] J.-S. Tang, Y.-L. Li, X.-Y. Xu, G.-Y. Xiang, C.-F. Li, and G.-C. Guo, Realization of quantum Wheelers delayed-choice experiment, Nat. Photonics **6**, 600 (2012).

[12] X.-S. Ma, J. Kofler, A. Qarry, and A. Zeilinger, Quantum erasure with causally disconnected choice, Proc. Natl. Acad. Sci. USA **110**, 1221 (2013).

[13] B. G. Englert, M. O. Scully, and H. Walther, Quantum erasure in double-slit interferometers with which-way detectors, Am. J. Phys. **67**, 325 (1999).

[14] U. Mohrhoff, Objectivity, retrocausation, and the experiment of Englert, Scully, and Walther, Am. J. Phys. **67**, 330 (1999).

[15] R. E. Kastner, The 'delayed choice quantum eraser' neither erases nor delays, Found. Phys. **49**, 717 (2019).

[16] R. L. Ingraham, Quantum nonlocality in a delayed-choice experiment with partial, controllable memory erasing, Phys. Rev. A **50**, 4502 (1994); Erratum **51**, 4295 (1995); S. Faetti, An alternative analysis of the delayed-choice quantum eraser, arXiv:1912.04101.

[17] Q. Guo, W.-J. Zhang, G. Li, T. Zhang, H.-F. Wang, and S. Zhang, Modified quantum delayed-choice experiment without quantum control or entanglement assistance, Phys. Rev. A **104**, 022210 (2021).

[18] B. R. La Cour and T. W. Yudichak, Classical model of delayed-choice quantum eraser, Phys. Rev. A **103**, 062213 (2021).

[19] R. Ionicioiu and D. Terno, Proposal for A Quantum Delayed-Choice Experiment, Phys. Rev. Lett. **107**, 230406 (2011).

[20] R. Ionicioiu, T. Jennewein, R. B. Mann, and D. R. Terno, Is wave-particle objectivity compatible with determinism and locality?, Nat. Commun. **5**, 4997 (2014).

[21] R. Rossi, Restrictions for the causal inferences in an interferometric system, Phys. Rev. A **96**, 012106 (2017).

[22] A. S. Rab, E. Polino, Z.-X. Man, N. Ba An, Y.-J. Xia, N. Spagnolo, R. Lo Franco, and F. Sciarrino, Entanglement of photons in their dual wave-particle nature, Nat. Commun. **8**, 915 (2017).

[23] A. Peruzzo, P. Shadbolt, N. Brunner, S. Popescu, and J. L. O'Brien, A quantum delayed-choice experiment, Science **338**, 634 (2012).

[24] F. Kaiser, T. Coudreau, P. Milman, D. B. Ostrowsky, and S. Tanzilli, Entanglement-enabled delayed-choice experiment, Science **338**, 637 (2012).

[25] S. B. Zheng, Y. P. Zhong, K. Xu, Q. J. Wang, H. Wang, L. T. Shen, C. P. Yang, J. M. Martinis, A. N. Cleland, and S. Y. Han, Quantum Delayed-Choice Experiment with A Beam Splitter in A Quantum Superposition, Phys. Rev. Lett. **115**, 260403 (2015).

[26] W. Qin, A. Miranowicz, G. Long, J. Q. You, and F. Nori, Proposal to test quantum wave-particle superposition on massive mechanical resonators, npj Quantum Inf. **5**, 1 (2019).

[27] R. Chaves, G. B. Lemos, and J. Pienaar, Causal Modeling the Delayed-Choice Experiment, Phys. Rev. Lett. **120**, 190401 (2018).

[28] H.-L. Huang, Y.-H. Luo, B. Bai, Y.-H. Deng, H. Wang, Q. Zhao, H.-S. Zhong, Y.-Q. Nie, W.-H. Jiang, X.-L. Wang *et al.*, Compatibility of causal hidden-variable theories with a delayed-choice experiment, Phys. Rev. A **100**, 012114 (2019).

[29] E. Polino, I. Agresti, D. Poderini, G. Carvacho, G. Milani, G. B. Lemos, R. Chaves, and F. Sciarrino, Device-independent test of a delayed choice experiment, Phys. Rev. A **100**, 022111 (2019).

[30] S. Yu, Y. N. Sun, W. Liu, Z. D. Liu, Z. J. Ke, Y. T. Wang, J. S. Tang, C. F. Li, and G. C. Guo, Realization of a causal-modeled

delayed-choice experiment using single photons, Phys. Rev. A **100**, 012115 (2019).
[31] M. Thenabadu and M. D. Reid, Leggett-Garg tests of macrorealism for dynamical cat states evolving in a nonlinear medium, Phys. Rev. A **99**, 032125 (2019).
[32] M. Thenabadu, G.-L. Cheng, T. L. H. Pham, L. V. Drummond, L. Rosales-Zárate, and M. D. Reid, Testing macroscopic local realism using local nonlinear dynamics and time settings, Phys. Rev. A **102**, 022202 (2020).
[33] M. Thenabadu and M. D. Reid, Bipartite Leggett-Garg and macroscopic Bell-inequality violations using cat states: Distinguishing weak and deterministic macroscopic realism, Phys. Rev. A **105**, 052207 (2022); M. D. Reid and M. Thenabadu, Weak versus deterministic macroscopic realism, arXiv:2101.09476.
[34] B. Yurke and D. Stoler, Generating Quantum Mechanical Superpositions of Macroscopically Distinguishable States via Amplitude Dispersion, Phys. Rev. Lett. **57**, 13 (1986).
[35] A. Leggett and A. Garg, Quantum Mechanics Versus Macroscopic Realism: Is The Flux there when Nobody Looks?, Phys. Rev. Lett. **54**, 857 (1985).
[36] J. S. Bell, On the Einstein-Podolsky-Rosen paradox, Physics **1**, 195 (1964).
[37] A. Einstein, B. Podolsky, and N. Rosen, Can Quantum-Mechanical Description of Physical Reality Be Considered Complete?, Phys. Rev. **47**, 777 (1935).
[38] M. D. Reid, Criteria to detect macroscopic quantum coherence, macroscopic quantum entanglement, and an Einstein-Podolsky-Rosen paradox for macroscopic superposition states, Phys. Rev. A **100**, 052118 (2019).
[39] D. Bohm, *Quantum Theory* (Constable, London 1951).
[40] J. Clauser and A. Shimony, Bell's theorem: Experimental tests and implications, Rep. Prog. Phys. **41**, 1881 (1978).
[41] N. Brunner, D. Cavalcanti, S. Pironio, V. Scarani, and S. Wehner, Bell nonlocality, Rev. Mod. Phys. **86**, 419 (2014).
[42] H. Jeong. M. Paternostro, and T. Ralph, Failure of Local Realism Revealed by Extremely-Coarse-Grained Measurements, Phys. Rev. Lett. **102**, 060403 (2009).
[43] H. Jeong, Y. Lim, and M. S. Kim, Coarsening Measurement References and the Quantum-to-Classical Transition, Phys. Rev. Lett. **112**, 010402 (2014).
[44] N. Brunner, S. Pironio, A. Acin, N. Gisin, A. A. Méthot, and V. Scarani, Testing the Dimension of Hilbert Spaces, Phys. Rev. Lett. **100**, 210503 (2008).
[45] R. Gallego, N. Brunner, C. Hadley, and A. Acín, Device-Independent Tests of Classical and Quantum Dimensions, Phys. Rev. Lett. **105**, 230501 (2010).
[46] J. Bowles, M. T. Quintino, and N. Brunner, Certifying the Dimension of Classical and Quantum Systems in a Prepare-and-Measure Scenario with Independent Devices, Phys. Rev. Lett. **112**, 140407 (2014).
[47] J. Ahrens, P. Badzi, A. Cabello, and M. Bourennane, Experimental device-independent tests of classical and quantum dimensions, Nat. Phys. **8**, 592 (2012).
[48] C. Wang *et al.*, A Schrödinger cat living in two boxes, Science **352**, 1087 (2016).
[49] M. Greiner, O. Mandel, T. Hånsch, and I. Bloch, Collapse and revival of the matter wave field of a Bose-Einstein condensate, Nature (London) **419**, 51 (2002).
[50] G. Kirchmair *et al.*, Observation of the quantum state collapse and revival due to a single-photon Kerr effect, Nature (London) **495**, 205 (2013).
[51] N. S. Williams and A. N. Jordan, Weak Values and the Leggett-Garg Inequality in Solid-State Qubits, Phys. Rev. Lett. **100**, 026804 (2008).
[52] A. N. Jordan, A. N. Korotkov, and M. Buttiker, Leggett-Garg Inequality with a Kicked Quantum Pump, Phys. Rev. Lett. **97**, 026805 (2006).
[53] L. Clemente and J. Kofler, Necessary and sufficient conditions for macroscopic realism from quantum mechanics, Phys. Rev. A **91**, 062103 (2015).
[54] J. J. Halliwell and C. Mawby, Conditions for macrorealism for systems described by many-valued variables, Phys. Rev. A **102**, 012209 (2020).
[55] J. P. Dowling, Quantum optical metrology–the low-down on high-N00N states, Contemp. Phys. **49**, 125 (2008).
[56] B. Opanchuk, L. Rosales-Zárate, R. Y. Teh, and M. D. Reid, Quantifying the mesoscopic quantum coherence of approximate NOON states and spin-squeezed two-mode Bose-Einstein condensates, Phys. Rev. A **94**, 062125 (2016).
[57] C. Emary, N. Lambert, and F. Nori, Leggett-Garg inequalities, Rep. Prog. Phys. **77**, 016001 (2014).
[58] G. C. Knee, K. Kakuyanagi, M.-C. Yeh, Y. Matsuzaki, H. Toida, H. Yamaguchi, S. Saito, A. J. Leggett, and W. J. Munro, A strict experimental test of macroscopic realism in a superconducting flux qubit, Nat. Commun. **7**, 13253 (2016).
[59] A. Palacios-Laloy, F. Mallet, F. Nguyen, P. Bertet, D. Vion, D. Esteve, and A. N. Korotkov, Experimental violation of a Bell's inequality in time with weak measurement, Nat. Phys. **6**, 442 (2010).
[60] J. Dressel and A. N. Korotkov, Avoiding loopholes with hybrid Bell-Leggett-Garg inequalities, Phys. Rev. A **89**, 012125 (2014).
[61] J. Dressel, C. J. Broadbent, J. C. Howell, and A. N. Jordan, Experimental Violation of Two-Party Leggett-Garg Inequalities with Semiweak Measurements, Phys. Rev. Lett. **106**, 040402 (2011).
[62] M. E. Goggin *et al.*, Violation of the Leggett-Garg inequality with weak measurements of photons, Proc. Natl. Acad. Sci. USA **108**, 1256 (2011).
[63] A. Asadian, C. Brukner, and P. Rabl, Probing Macroscopic Realism via Ramsey Correlation Measurements, Phys. Rev. Lett. **112**, 190402 (2014).
[64] C. Budroni, G. Vitagliano, G. Colangelo, R. J. Sewell, O. Gühne, G. Tóth, and M. W. Mitchell, Quantum Nondemolition Measurement Enables Macroscopic Leggett-Garg Tests, Phys. Rev. Lett. **115**, 200403 (2015).
[65] L. Rosales-Zárate, B. Opanchuk, Q. Y. He, and M. D. Reid, Leggett-Garg tests of macrorealism for bosonic systems including two-well Bose-Einstein condensates and atom interferometers, Phys. Rev. A **97**, 042114 (2018).
[66] R. Uola, G. Vitagliano, and C. Budroni, Leggett-Garg macrorealism and the quantum nondisturbance conditions, Phys. Rev. A **100**, 042117 (2019).
[67] J. Halliwell, A. Bhatnagar, E. Ireland, H. Nadeem, and V. Wimalaweera, Leggett-Garg tests for macrorealism: Interference experiments and the simple harmonic oscillator, Phys. Rev. A **103**, 032218 (2021).

[68] A. K. Pan, Interference experiment, anomalous weak value, and Leggett-Garg test of macrorealism, Phys. Rev. A **102**, 032206 (2020).
[69] L. Rosales-Zarate, R. Y. Teh, S. Kiesewetter, A. Brolis, K. Ng, and M. D. Reid, Decoherence of Einstein–Podolsky–Rosen steering, J. Opt. Soc. Am. B **32**, A82 (2015).
[70] M. D. Reid, Interpreting the macroscopic pointer by analysing the elements of reality of Schrödinger cat, J. Phys. A: Math. Theor. **50**, 41LT01 (2017).
[71] M. Brune, E. Hagley, J. Dreyer, X. Maître, A. Maali, C. Wunderlich, J. M. Raimond, and S. Haroche, Observing the Progressive Decoherence of the 'Meter' in a Quantum Measurement, Phys. Rev. Lett. **77**, 4887 (1996).
[72] C. Monroe, D. M. Meekhof, B. E. King, and D. J. Wineland, A 'Schrödinger cat' superposition state of an atom, Science **272**, 1131 (1996).
[73] F. Fröwis, P. Sekatski, W. Dür, N. Gisin, and N. Sangouard, Macroscopic quantum states: measures, fragility, and implementations, Rev. Mod. Phys. **90**, 025004 (2018).
[74] M. D. Reid, Demonstration of the Einstein-Podolsky-Rosen paradox using nondegenerate parametric amplification, Phys. Rev. A **40**, 913 (1989).
[75] M. D. Reid, P. D. Drummond, W. P. Bowen, E. G. Cavalcanti, P. K. Lam, H. A. Bachor, U. L. Andersen, and G. Leuchs, The Einstein-Podolsky-Rosen paradox: From concepts to applications, Rev. Mod. Phys. **81**, 1727 (2009).
[76] E. G. Cavalcanti, P. D. Drummond, H. A. Bachor, and M. D. Reid, Spin entanglement, decoherence and Bohm's EPR paradox, Opt. Express **17**, 18693 (2009).
[77] H. M. Wiseman, S. J. Jones, and A. C. Doherty, Steering, Entanglement, Nonlocality and the Einstein-Podolsky-Rosen Paradox, Phys. Rev. Lett. **98**, 140402 (2007).
[78] S. J. Jones, H. M. Wiseman, and A. Doherty, Entanglement, Einstein-Podolsky-Rosen correlations, Bell nonlocality, and steering, Phys. Rev. A **76**, 052116 (2007).
[79] E. G. Cavalcanti, S. J. Jones, H. M. Wiseman, and M. D. Reid, Experimental criteria for steering and the Einstein-Podolsky-Rosen paradox, Phys. Rev. A **80**, 032112 (2009).
[80] R. Uola, A. C. S. Costa, H. C. Nguyen, and O. Gühne, Quantum Steering, Rev. Mod. Phys. **92**, 015001 (2020).
[81] R. Y. Teh, L. Rosales-Zárate, B. Opanchuk, and M. D. Reid, Signifying the nonlocality of NOON states using Einstein-Podolsky-Rosen steering inequalities, Phys. Rev. A **94**, 042119 (2016).
[82] S. Slussarenko, M. M. Weston, H. M. Chrzanowski, L. K. Shalm, V. B. Verma, S. W. Nam, and G. J. Pryde, Unconditional violation of the shot-noise limit in photonic quantum metrology, Nat. Photonics **11**, 700 (2017).
[83] D. M. Greenberger, M. A. Horne, and A. Zeilinger, *Bell's Theorem, Quantum Theory, and Conceptions of the Universe* (Kluwer, Dordrecht, 1989), p. 69.
[84] M. D. Reid and W. J. Munro, Macroscopic Boson States Exhibiting the Greenberger-Horne-Zeilinger Contradiction with Local Realism, Phys. Rev. Lett. **69**, 997 (1992).
[85] A. Cabello, Multiparty multilevel Greenberger-Horne-Zeilinger states, Phys. Rev. A **63**, 022104 (2001).
[86] W. Son, Jinhyoung Lee, and M. S. Kim, Generic Bell Inequalities for Multipartite Arbitrary Dimensional Systems, Phys. Rev. Lett. **96**, 060406 (2006).
[87] A. L. O. Bilobran and R. M. Angelo, A measure of physical reality, Europhys. Lett. **112**, 40005 (2015).
[88] F. R. Lustosa, P. R. Dieguez, and I. G. da Paz, Irrealism from fringe visibility in matter waves double-slit interference with initial contractive states, Phys. Rev. A **102**, 052205 (2020).
[89] P. Milman, A. Auffeves, F. Yamaguchi, M. Brune, J. M. Raimond, and S. Haroche, A proposal to test Bell's inequalities with mesoscopic non-local states in cavity qed, Eur. Phys. J. D **32**, 233 (2005).
[90] Z. Leghtas, G. Kirchmair, B. Vlastakis, M. H. Devoret, R. J. Schoelkopf, and M. Mirrahimi, Deterministic protocol for mapping a qubit to coherent state superpositions in a cavity, Phys. Rev. A **87**, 042315 (2013).
[91] H.-Y. Ku, N. Lambert, F.-J. Chan, C. Emary, Y.-N. Chen, and F. Nori, Experimental test of non-macrorealistic cat states in the cloud, npj Quantum Inf. **6**, 98 (2020).